Short heat shock has a long-term effect on mesenchymal stem cells' transcriptome

Ivana Ribarski-Chorev[1], Gisele Schudy[1], Carmit Strauss[1], Sharon Schlesinger[1]

[1]The Robert H. Smith Faculty of Agriculture, Food and Environment, The Hebrew University of Jerusalem, Israel

Correspondence:

Dr. Sharon Schlesinger: sharon.shle@mail.huji.ac.il

Keywords

Heat shock, bovine, mesenchymal stem cells, transcriptome, stress, bivalent genes, umbilical cord.

Running title:

Transcriptional changes following heat shock

Summary blurb

Heat shock alters mesenchymal stem cells' transcriptional programs, resulting in stable activation of lineage commitment genes, thus explaining the shift in the identity and fate of the cells.

Graphical abstract

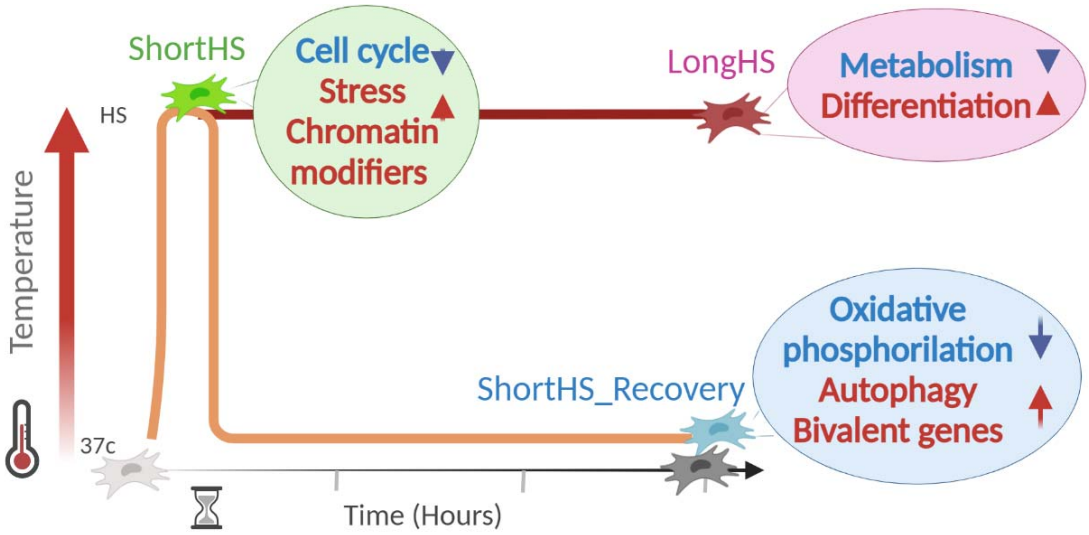

Abstract

The harmful consequences of heat stress (HS) on physiology are well documented, but the molecular aspects of changing thermal conditions are poorly understood. Therefore, a better understanding of the effects of this stress on the morphology, phenotype, proliferative capacity, and fate decision of MSCs is required. Our thorough characterization of MSCs' transcriptome showed a major effect of HS on the transcriptional landscape. Specifically, examining the effect after three days of moderate HS shows changes in many cell processes, such as immune response, cell cycle, and differentiation. Surprisingly, we detected a long-term effect on cell identity even after short stress, possibly through the activation of bivalent genes related to cell lineage decisions. Finally, comparing the differentially expressed genes following short HS with their transcriptional state after three days of recovery, we find transient upregulation of many members of the MLL family and other histone modifiers; a finding which offers a potential mechanistic account for the stable bivalent genes activation. This could be used to predict and modify the long-term effect of HS on cell identity.

Introduction

Environmental stressors harm human and animal health around the world (Peters et al., 2021; Richter et al., 2010). Heat exposure in particular is an increasing problem as climate change progresses; exposures to extreme temperatures vastly affect the organism as a whole and on the cellular level. Adverse effects of heat stress in humans include heat stroke, systemic inflammation, nervous system impairment, adverse birth outcomes, global DNA methylation, and telomere shortening (Peters et al., 2021). In animals, heat stress was found to have detrimental effects on fertility and well-being (Agarwal et al., 2014; de Barros & Paula-Lopes, 2018; Kitagawa et al.,

45 2004). In cattle, the frequency of many chronic inflammation-related diseases is elevated during
46 hot periods (Chen et al., 2018; Olde Riekerink et al., 2007), resulting in reduced animal welfare and
47 significant economic losses to the dairy industry (Key et al., 2014). In-utero heat stress in cattle
48 was recently found to reduce placental weight, blood flow, birth weight, and innate and cellular
49 immunity (Dado-Senn et al., 2020). Moreover, heat stress has a long-term effect on oocyte
50 developmental capacity and follicular steroidogenesis in cattle and other mammals (Kawano et al.,
51 2022; Roth, 2017). It has been suggested that alterations of the cellular epigenetic landscape are
52 responsible for these persisting effects (de Barros & Paula-Lopes, 2018; Sharma & Bhonde, 2020;
53 Xue & Acar, 2018).

54 On a cellular level, thermal stress is associated with oxidative stress, endoplasmic reticulum (ER)
55 stress, and neurochemical stress, and impairs protein folding, cell cycle, and mitochondrial
56 function (Agarwal et al., 2014; Chen et al., 2018; Kitagawa et al., 2004; Shimoni et al., 2020). On
57 the transcriptional level, cells exposed to HS generally activate a cascade of heat shock proteins and
58 factors which in turn regulate downstream pathways that protect the stressed cells. The effect of
59 external temperature has been examined in various animals and tissues such as bovine PBMCs
60 (Garner et al., 2020), mammary tissues (Collier et al., 2006; Yue et al., 2020) and granulosa cells
61 (Sammad et al., 2022). Another study exposed rats to heat stress and examined the transcriptional
62 changes in 3 different tissues (Dou et al., 2021). Although many key genes and pathways that
63 respond to acute thermal stress were identified in these studies, only a few genes were common
64 across tissues, suggesting a high level of tissue specificity in the transcriptional response to thermal
65 stress.

66 Heat stress effects on adult stem cells are of special interest. These cells are the longest-living
67 proliferative cells in multicellular organisms (Schultz & Sinclair, 2016); hence they have an

68 increased risk of accumulating genetic and metabolic damage. Extrinsic factors including
69 environmental stress can enhance this damage accumulation, possibly leading to the functional
70 decline of the stem cells (Ermolaeva et al., 2018). Mesenchymal stromal cells (also called
71 mesenchymal stem cells, MSCs) are a heterogeneous group of non-hematopoietic multipotent stem
72 cells that assist in the preservation of homeostasis in many organs and tissues (Pittenger et al.,
73 1999). Additionally, physiological MSC stores are essential for the regeneration of many tissues in
74 the body, acting through common signaling pathways such as Wnt, BMP, and Notch (Naaldijk et
75 al., 2015). Cultured MSCs are most frequently derived from adult tissue sources such as bone
76 marrow and adipose tissue or from birth-associated tissue such as placental tissue, amniotic
77 membranes, and umbilical cord (Hass et al., 2011; Nowakowski et al., 2016). When grown in
78 culture, MSCs can self-renew, differentiate into several tissues, and modulate the immune
79 response in their surroundings (Dominici et al., 2006; Kuroda & Dezawa, 2014; Uccelli et al.,
80 2008). When activated, MSCs secrete biologically active compounds and generate exosomes that
81 modify the function of their cellular microenvironment (Kou et al., 2022; Madrigal et al., 2014;
82 Phinney & Pittenger, 2017). Due to these characteristics, MSCs are commonly suggested as
83 candidates for cell-based therapy or as the cell source for tissue engineering and cultured meat
84 products. However, it is still unclear how the properties and key biological functions of MSCs *in*
85 *vitro* are influenced by parameters such as cell source, culture conditions, and environmental
86 factors, including heat stress. Indeed, the long-term epigenetic effects of variations in culture
87 conditions are only beginning to be uncovered (Isik et al., 2021; Sharma & Bhonde, 2020). An
88 example of such an effect is hypoxia-preconditioning, which was shown to significantly reduce
89 global 5hmC in swine MSCs but had no effects on H3K4me3, H3K9me3, or H3K27me3 (Isik et al.,
90 2021). Overall, the long-term effects of stress on MSCs are barely characterized.

91 Here, we set out to evaluate the immediate and long-term effects of HS treatment on the bovine
92 umbilical cord (bUC)-derived MSC transcriptome. In our previous study, we demonstrated that HS
93 treatment changed the proliferation, differentiation, and immunomodulatory potential of bUC-
94 MSCs (Shimoni et al., 2020). Several HS protocols were shown to have the common effect of
95 reducing proliferation and inducing oxidative stress and premature senescence. However, each HS
96 protocols showed profound variation in gene expression and immunomodulatory potential.
97 Surprisingly, even one hour of treatment at 42°C had a long-term effect on bUC-MSCs function
98 and transcriptional pattern 3 days after the HS, which partially persisted even after eleven
99 passages (about 40 days) in culture (Shimoni et al., 2020). However, at temperatures higher than
100 41°C the survival rate of mammalian cells decreases with increasing exposure time (Asseng et al.,
101 2021; Moise et al., 2018). Here, to gain an unbiased view of the cell-intrinsic response to heat
102 shock, we performed gene expression profiling using RNA sequencing (RNA-Seq) following
103 exposure of the bUC-MSCs to moderate HS (40.5^{o}C) of different lengths. We hypothesize that
104 transcriptional response to heat stress has two manifestations: a major immediate and transitory
105 reaction of stress response-related genes, and a minor but permanent response of epigenetically
106 altered transcripts. By examining the transcriptional response and functionality of MSCs after mild
107 HS, this work will advance our understanding of the short- and long-term impacts of thermal
108 stress on the organismal stem cell pool.
109
110 **Results**
111 ***RNA-seq analysis of heat shock treated and control cells.***
112 To examine the effects of thermal stress on the cell's transcriptome, we evaluated the
113 transcriptional response of MSCs to *in vitro* heat shock (HS). MSCs were extracted from the UC of
114 a preterm fetus as previously described (Shimoni et al., 2020). Prior to the HS treatment, MSCs

115 marker expression (Supplementary Figure S1A), proliferation (Supplementary Figure S1B), and
116 differentiation capacities (Supplementary Figure S1C) were examined and validated as in (Nir &
117 Ribarski-Chorev et al., 2022; Shimoni et al., 2020).
118 HS treatment protocols were designed to examine the short- or long-term effects of exposure to
119 mild HS conditions (Figure 1A). One day after seeding MSCs from early passages (P2–P4), were
120 moved from 37°C to 40.5°C for six-hour (ShortHS) or three days (LongHS) or a six hours HS
121 followed by three days recovery back at 37°C (ShortHS_Recovery). Each HS treatment had a
122 matching 37°C normothermic (NT) control (ShortNT and LongNT). The two time points were
123 selected to capture the immediate transcriptional effects of HS vs. the stable and delayed ones.
124 Immediately after the completion of the six hours or three days treatments, the cells were
125 harvested, viability was checked and pellets were stored at -80° for later matched RNA extraction
126 and sequencing. The viability of the cells and their MSC marker expression levels remained high
127 following the various treatment protocols (Supplementary Figure S1D, S1E). Two or three
128 biological repeats were done for each treatment (Supplementary Table S2). All RNA samples were
129 run together on Nextseq Illumina and showed a high percentage and quality of mapping to exons
130 and low levels of rRNA and mitochondrial DNA contaminations (Supplementary Figure S2A, S2B).
131 Principal component analysis shows that the HS treatment determined the transcriptome profile
132 as samples from the same treatment clustered together and apart from the other treatment groups
133 (Figure 1B). Hierarchical clustering uncovered a secondary factor affecting the transcriptome
134 which could be attributed to the time passed from seeding (Supplementary Figure S2C) or the
135 population doubling (Supplementary Table S3). Several genes were also evaluated by RT-qPCR to
136 validate the sequencing results (Supplementary Figure S2D).

137 We found that the various HS treatments significantly changed the expression levels of a total of
138 3667 genes (padj ≤0.05 and log2(FC)≥1) (Figure 1C). After six hours of HS, 712 differentially
139 expressed genes (DEGs) were found, whereas after three days of HS 1,371 DEGs were found, most
140 of them downregulated (Supplementary Figure S2E). In the cells that were allowed to recover at
141 37°C for three days after the short HS, 2,037 genes were changed versus the short HS. However,
142 only a slight difference is found when compared to the long NT sample. This suggests that after a
143 short HS there is a major recovery from the stress, at least on the transcriptional level. The results
144 indicate that short thermal shock affects MSCs' gene expression rapidly and widely but mostly
145 transiently.
146 To discern the dominant systematic changes following the different HS treatments, we performed
147 k-means clustering on all 3,667 DEGs (Figure 1D and Supplementary Figure S3). The resulting
148 clusters revealed three major modes of change. Clusters 2 and 4 show the common effect of both
149 long and short HS on the transcriptional pattern. Conversely, in clusters 3 and 7 the change is only
150 observed after the long HS, portraying that more genes were induced after three days, possibly due
151 to a slower transcriptional response rate (Figure 1C). Clusters 1 and 6 show the effect of culturing
152 time on the transcriptional pattern.
153 While changes in expression patterns are evident from the k-means clustering analysis, we wanted
154 to systematically examine the transcriptional changes following each treatment alone and identify
155 specific biological features and processes.
156 ***Cell cycle and immune response are downregulated as developmental pathways are activated***
157 ***following a long heat shock***
158 To get a comprehensive understanding of all the changes that occurred following the HS, we
159 delved into the analysis of each treatment using the gene set enrichment analysis (GSEA) and gene

160 ontology (GO) tools (as described in the supplementary materials and methods). First, we focused
161 on the changes observed in cells exposed to long HS vs. long NT control (Figure 2A). On the
162 morphological level, cells appeared flattened, with expanded cytoplasm and detectable stress
163 granules (Figure 2B, stress granules marked with arrows). On the transcriptional level, 1,371 DEGs
164 (padj ≤0.05 & log2(FC)≥1) were found (Figure 1C). GSEA analysis show downregulation of cell
165 proliferation and metabolism; namely cell cycle and DNA repair, glycolysis and oxidative
166 phosphorylation (Figure 2C and Supplementary Figure 4A) and upregulated response to stress
167 (Figure 2C). Interestingly, many differentiation and cell-fate related pathways (Figure 2D,
168 Supplementary Figure 4B, C) were also upregulated, as previously suggested (Khan et al., 2020).
169 For example, general terms of cell growth and morphogenesis were enriched, as well as more
170 specific terms like connective tissue, chondrocytes, osteoblasts, kidney, and neuronal system are
171 upregulated. In addition, there is apparent upregulation of cell adhesion molecules, which
172 represents cell-cell interactions and the interaction between the cell and the extracellular matrix
173 (ECM). These molecules promote a broad spectrum of cell signaling that directly or indirectly
174 modulates stem cell proliferation, self-renewal property, adhesion, and multilineage differentiation
175 (Abdal Dayem et al., 2018; Stopp et al., 2013). There is downregulation of gene sets related to
176 inflammation and the immune system, as well as DNA damage and ROS response. This could be
177 explained by the long duration of the HS, which might have required the cells to attenuate their
178 stress response. What is more, these changes were accompanied by the upregulation of post-
179 translational modifiers, specifically histone demethylases and Polycomb group (PcG) complex
180 members (Figure 2E). Additionally, KEGG analysis showed enrichment and upregulation of
181 pathways such as MAPK, PI3K-Akt, RAS and RAP1 (Figure 2F). In general, those pathways are
182 known to regulate cell size, survival, differentiation, adaptation to growth conditions, and stress

183 responses (Li et al., 2017). PI3K-Akt activates the mTOR signaling pathway (Li et al., 2017; Su &
184 Dai, 2017), which is also elevated following heat stress in bovine granulosa cells (Khan et al.,
185 2020). Activation of PI3K-Akt and mTOR pathways plays a central role in cellular senescence and
186 organismal aging and thus acts as a driver of stem cell depletion and reduced tissue regenerative
187 capacity (Antonioli et al., 2019; Johnson et al., 2013; Saxton & Sabatini, 2017).
188 In summary, our data demonstrate that three days of HS treatment are not detrimental to cell
189 viability but have a major effect on cell fate and aging. Although the impact of long HS on
190 differentiation might prove useful as a pretreatment protocol for MSC transplantations, this
191 duration of HS is scarcely experienced in physiological settings. Hence, we wished to examine the
192 effect of short (six hours) HS on the MSCs.
193 ***Stress responses are induced while cellular functions decline following a short heat shock***.
194 Initially, we focused on the immediate effects of short HS (Figure 3A) using GSEA analysis. Five
195 out of the ten most upregulated genes in this treatment (HSPA1A, HSPA6, HSPA4L, HSPB1, HSPH1,
196 Figure 3B) were heat stress genes, along with genes that regulate redox maintenance (SLC27A5),
197 insulin levels (MAFA) and mitotic progression (MISP). The most downregulated genes following
198 short HS are involved in RNA interference (RNAi) process (TSNAX), post-splicing multiprotein
199 complex (UPF3A), cell polarity (DAAM2), metabolism regulation (DHRSI2) and chromatin and
200 transcription process (H1-2). These genes are mostly included in the Hallmark gene sets that are
201 enriched for up- and down- regulated processes following six hours of HS (Figure 3C and
202 Supplementary Figure 5A, 5B). Short heat stress induced stress response and differentiation
203 pathways while halting oxidative phosphorylation and cell cycle. Upregulated biological processes
204 enriched in GSEA were stress response, autophagy, development, and mRNA transcription (Figure
205 3D, Supplementary Table S4), while downregulated processes were all related to DNA replication

206 (Figure 3E and Supplementary Figure 5B). In addition to GSEA, we performed the analysis in
207 g:Profiler, KEGG and Reactome which also suggests that stress response and ER activity were
208 induced whereas DNA replication, with an emphasis on initiation, was decreased (Figure 3F). After
209 discovering dramatic short-term changes, we proceeded to check how many of these changes
210 remained stable. To elucidate these stable changes, the treated cells were allowed to recover in
211 normothermia for three days before the transcriptional analysis.

212 ***Long term effects of short heat stress.***

213 To identify the transcriptional changes which occurred after short HS but remained stable even
214 after 3 days of recovery, we compared the three different time points: control (as the zero-time
215 point), six hour HS and six hour HS followed by three days of recovery (ShortNT vs. ShortHS vs.
216 ShortHS_Recovery, Figure 4A). Thus, we re-analyzed the data (see Supplementary materials and
217 methods) using K-means clustering to visualize transcriptomic differences (Figure 4B). While after
218 recovery most genes regained similar expression levels to that of the control sample, two clusters
219 in which the differential expression persisted were identified. Cluster 2 genes were lowly expressed
220 in the control sample but were then upregulated after the short HS and remained active after
221 recovery. GO annotations and KEGG pathways enriched in this cluster are mostly related to stress
222 and protein degradation (Figure 4C). This implies that some elements of the stress response to
223 acute stress last for more than three days. Cluster 3 is the mirror image of cluster 2, presenting
224 stably downregulated genes related to proliferation and metabolism but also senescence and DNA
225 damage (Figure 4D). This might suggest that following short HS, the cells enter a state of
226 quiescence to maintain their stemness. This data is in agreement with our population doubling
227 time analysis, which shows slower proliferation after both the long and the short HS (Figure 4E).

228 Similar analysis done on the other two clusters, 1 and 4, raised an interesting point. Of the most 25
229 significantly enriched GO terms in cluster 4, only 3 are not related to transcriptional regulation,
230 mostly epigenetic modification (Figure 4F). This raised the intriguing hypothesis that the
231 epigenetic landscape is altered following the short HS, possibly with long term consequences. To
232 examine how a short period of stress could have that kind of persistent effect, we used the
233 EpiFactors Database (Medvedeva et al., 2015) and related MGI annotations to identify enriched
234 epigenetic modifiers in the data. Several epigenetic complexes were found highly enriched in
235 Cluster 4, i.e., upregulated after six hour HS and then back to low expression after recovery
236 (Figure 4G). Interestingly, those complexes are all related to the mixed lineage leukemia (MLL)
237 proteins which catalyze the trimethylation of histone H3 Lys 4 (H3K4me3), a mark associated with
238 active or poised transcription and found in the promoters of most active or poised genes
239 (Harikumar & Meshorer, 2015). Bivalent genes are lineage-specification genes that carry both
240 H3K4me3 and H3K27me3 histone marks and are regulated by the balance between the two
241 histone marks. This balance is mediated by PcG members and the MLL coactivator complex (Noer
242 et al., 2009). We searched for known targets of the MLL complex in our list and found cluster 2
243 (i.e. upregulated in both short- and long-term) to be significantly enriched for bivalent genes (Mas
244 et al., 2018) crucial to cell fate regulation: several FGF family members, FZD3, JUN, FOXF1, VEGFA
245 and KDM6B, to state a few (Supplementary Figure S6). This was in contrast to the other clusters,
246 where these and other bivalent genes were significantly underrepresented (Figure 4H). Overall,
247 this data sheds light on the long-term effects of short HS and suggests that a short stress event can
248 modulate the epigenetic regulation of key cell fate genes.
249 Next, we wished to uncover the transcriptional changes shared by all HS-treated cells.
250 ***Key characteristics of MSC vary with heat stress duration.***

251 So far, we have shown considerable effects of short and long HS *in vitro*. To examine to what
252 extent the DEGs are shared between the timepoints, we had to eliminate the effect of culturing
253 time and the circadian clock and focus solely on the effect of HS. To that end, we removed all DEGs
254 that changed between the short and long NT controls (see Supplementary materials and methods
255 for the analysis) and examined which DEGs were commonly upregulated (Figure 5A) or
256 downregulated (Figure 5B) in all HS. A total of 102 upregulated and 93 downregulated DEGs were
257 shared by short and long HS treatments, a highly significant enrichment over what could be
258 expected by chance. While the commonly upregulated genes were mostly related to stress
259 response, the commonly downregulated genes were not significantly enriched to any specific
260 pathway or process. Hence, we examined if the different DEGs are annotated to shared biological
261 processes and pathways which are therefore affected by both short and long HS. Important cellular
262 functions like oxidative phosphorylation and cell cycle were found to be impaired in all HS;
263 immune system was downregulated, and the hedgehog signaling pathway was significantly
264 upregulated following HS, even after the recovery period (Figure 5C, Supplementary Figures S7A-
265 D).
266 To understand the effect of HS on the biological processes related to the key capacities of MSCs,
267 namely self-renewal, differentiation and immunomodulation, we compared the relevant biological
268 processes and functions between different treatments. For cell cycle we saw that while in all three
269 treatments the downregulated DEGs were enriched for the general term 'cell cycle', only the short
270 HS is downregulating specifically DNA replication pre-initiation (e.g., genes like MCM2 and 7,
271 CDC6 and E2F1). The three days samples showed downregulation of genes required for the G2/M
272 phase (namely cyclin A and B and CDC25), suggesting a block before mitosis (Figure 5D).
273 Interestingly, the cells that got the short HS but were let to recover for three days in normothermia

274 show both the G1/S and the G2/M effects although to a lesser degree, suggesting that even short
275 thermal stress might disrupt cell cycle regulation and proliferation. These results are supported by
276 the population doubling we saw in the culture following the experiments (Figure 4E) as well as in
277 our previously described cell cycle analysis (Shimoni et al., 2020).
278 As for differentiation, it appears that several developmental pathways were activated, depending
279 on the heat shock treatment (Figure 5E, Supplementary Figure S7E-F). The long HS induced
280 various differentiation pathways; the most enriched were the differentiation to
281 mesoderm/mesenchymal fate. Notably, both canonical and non-canonical WNT pathways were
282 upregulated after long HS, suggesting a general shift in cell identity. The short HS upregulates the
283 canonical WNT but downregulates the non-canonical (WNT5a related) pathway (Figure 5E,
284 Supplementary Figures S7E, F). In line with the fact that KEGG definitions like "canonical WNT
285 pathway" includes both activators and suppressors, this and other pathways are enriched in both
286 the down and upregulated DEGs. Interestingly, HOX genes related to skeletal morphogenesis and
287 several epigenetic factors (e.g., Setd2, Kdm6a, Jarid1) were upregulated following both long and
288 short HS; suggesting that heat shock treatment may slow proliferation while promoting MSC's
289 commitment and differentiation.
290 Immunomodulatory properties of MSCs have previously been shown to decline following stress
291 (Bagath et al., 2019; Shimoni et al., 2020). Major downregulation of immune related pathways was
292 detected after HS (Figure 5F). GO analysis in GSEA revealed considerable effects on the production
293 of interleukins (ILs), TNFs and INF-ɤ. In addition, we observed the downregulation of antigen
294 processing, acute inflammatory response, response to chemokines, and the migration and
295 chemotaxis of macrophages, neutrophils, and granulocytes (Supplementary Table S5). The list of
296 760 genes in the "Cytokine Signaling in Immune system SuperPath"

297 (https://pathcards.genecards.org) was analyzed and 38 of them (for example IL1Rs, IL7 and IL18)
298 were downregulated after long HS while 17 (like FGF2 and FGFR2 which are related to
299 differentiation (Khalid et al., 2021; Zhang et al., 2022)), are upregulated (Figure 5G). Overall, genes
300 related to IL production are significantly downregulated (hypergeometric p-value = 2.49e-04,
301 Figure 5G).

302 **Discussion**

303 Here, we show that the transcriptional changes following heat shock *in vitro* are broad and can
304 alter every functional aspect of MSC identity. We analyzed RNA-seq from bUC-MSCs in
305 normothermia vs. short or long exposures to HS, to investigate the subsequent changes in the
306 transcriptional landscape that might lead to a shift in the cell's identity and fate. We were
307 particularly interested in identifying the long-term effect of thermal stress on cell proliferation,
308 differentiation, and immunomodulation capacities; as those key MSC features were amongst the
309 most abundant GO term groups. To examine the relevance of our data to physiological heat stress,
310 we compared our DEGs to a list of 55 genes defined as thermal stress responsive in a bovine study
311 done *in vivo* (Fang et al., 2021): 36 of the 55 genes were found to be differentially expressed
312 following short, long or both HS groups. The genes EIF2A, HSPA1A, HSP90AA1, and HSF1 were
313 considered by the authors key genes that responded to thermal stress of Holstein dairy cattle.
314 From our experiments, HSPA1A, and HSP90AA1 were indeed upregulated DEGs for short and long
315 HS groups, and EIF2A for shortHS group only. HSF1 was not differentially expressed in our
316 treatments, maybe due to our use of 40.5°C which is mild relative to the 42°C used by the authors.
317 In addition, Fang et al. bioinformatics analyses pinpointed biological processes and pathways
318 associated with thermal stress that are very similar to those we have identified, e.g., protein

319 folding, transcription factor binding, immune effector process, negative regulation of cell
320 proliferation, PI3K- Akt signaling pathway, and MAPK signaling pathway.
321 The immediate transcriptional changes found following short HS include the onset of several
322 cellular stress responses and cell cycle arrest in G1/S. This checkpoint arrest is a known adaptive
323 cellular response to heat stress, in which cells slowdown proliferation rate while rapidly upregulate
324 the transcription and translation of HSPs to maintain cell homeostasis and retain their cellular
325 functions (Richter et al., 2010). Our previous results, which showed cell cycle arrest at G1/S after
326 short HS (Shimoni et al., 2020) also support this finding. Two possible interpretations arise, each
327 with a different implication for stemness and differentiation: in one, following the short HS the
328 cells enter a quiescent state; this is in alignment with the observed metabolic changes (reduced
329 amino acid metabolism, reduced oxidative phosphorylation, increased glycolysis, and mitophagy
330 induction of mitochondrial renewal, etc.), as reviewed in (van Velthoven & Rando, 2019). This
331 suggest that short HS treatment encourages the retention of MSC stemness. In the other
332 interpretation, a long G1 may allow for the accumulation of the epigenetic changes needed for the
333 initiation of fate decisions (Dalton & Coverdell, 2015). This interpretation might explain the
334 transient upregulation of many epigenetic factors and the stable changes in many lineage
335 commitment genes observed after three days recovery. To mechanistically challenge those two
336 interpretations and to determine whether HS promotes stemness or differentiation, further study,
337 preferably on the single cell level, is required to mechanistically challenge these two
338 interpretations.
339 Evident changes were observed in the morphology and proliferation rate of the cells three days
340 after the Short or Long HS treatment. However, on the transcriptional level, the majority of
341 ShortHS DEGs reverted to normal expression levels after three days recovery, and only a subset of

342 the DEGs remained. In this subset of stable DEGs we see the upregulation of several developmental
343 genes known as "bivalent" for their dual histone lysine tri-methylation marking in both K4 (active
344 mark) and K27 (repressive mark). Those genes are known targets of the MLL complex, which
345 carries out the methylation of histone H3 lysine 4 and was transiently overexpressed after the
346 initial HS event. So, a sequence of events can be hypothesized. First, the short HS upregulates the
347 MLL complex members, thus shifting the balance between the active and repressive histone marks.
348 Consequently, the chromatin of the previously poised (and silent) bivalent genes opens to enable
349 transcription of developmental genes, priming the cells toward cell fate determination. Evaluation
350 of this hypothesis will require follow-up studies examining changes in epigenetic marking
351 following HS.
352 The idea that cells after HS pretreatment are more prone to differentiation is tempting. If indeed
353 priming MSCs by specific stress can help us direct their fate, it could provide us with another tool
354 in the cellular therapy toolbox. Moreover, as the idea of cellular agriculture, or cultured meat, gains
355 increasing attention, more cost effective and clean ways to differentiate the source cells toward the
356 intended fate (usually muscle or fat) are needed. Current differentiation protocols require large
357 amounts of expensive and unstable growth factors, which raise costs and hinder
358 commercialization of cultured meat. Every pretreatment protocol that is easy, cheap, and reduces
359 the time and resources necessary for differentiation, will have huge economic and environmental
360 consequences.
361 On the clinical level it is interesting to note the negative effect of long HS on MSC immune activity,
362 possibly compromising the cells' immunomodulatory functions. Indeed, reduced
363 immunomodulation was previously observed when we co-cultured MSCs subjected to HS with
364 macrophages (Shimoni et al., 2020). The reduced immunomodulation capacity of the stressed

365 MSCs might account for the increased production of inflammatory cytokines found in mammary
366 epithelial cells following HS (Gao et al., 2019). Hence, the increased rates of inflammatory diseases
367 in dairy cows during the summer months could be partially attributed to the failure of the
368 malfunctioning MSCs to modulate the inflammatory response of the surrounding cells to HS.
369 Overall, identifying the long-term effect of HS on MSC capacities suggest an explanation for the
370 seeming contradiction between the in vitro experiments which show beneficial effects to HS
371 priming and the in vivo data that demonstrate harmful physiological consequences to thermal
372 stress (reviewed by (Roth, 2020)).
373 Although we have demonstrated that HS affects MSCs' transcriptome, our study has some
374 limitations. Population heterogeneity, circadian clock, culturing time, and culture conditions all
375 have effects on RNA-seq results that need to be controlled for (Supplementary Figure S8). To
376 counter this drawback we (1) made sure that at the end of the experiment (either six hours or 3
377 days) all the treatment groups had similar culture density (Supplementary Table S2) (2) sequenced
378 two or three independent biological repeats from each treatment group (Supplementary Table S3)
379 (3) to reduce heterogeneity that might originate in genetic background, the same MSC line was
380 used in all three repeats. To counter the effects of culturing time, we used untreated (NT) controls,
381 one for the short HS, and the other for the long HS. When we compared gene expression at the
382 short and long time points, all DEGs that were apparent between the NT control time points (and
383 were assumed to be the result of culturing effect) were ignored. Interestingly, two transcription
384 factors regulating the circadian clock, BHLHE40 and TIMELESS, were found among those ignored
385 DEGs. These two transcription factors together regulate the expression of 202 other DEGs in this
386 group (Supplementary Figure S8B). These oscillating genes may partly explain the relatively high
387 number of DEGs due to culturing effect since the ShortHS and ShortNT samples were taken at

388 noon (24h after seeding + six hours treatment) while the three day samples (LongHS, LongNT and
389 ShortHS_Recovery) were collected in the morning (exactly 96h after seeding).

390 **Conclusions**

391 The use of MSCs for cell therapy or cultured meat has several advantages, such as high availability,
392 low production price, and fast and easy differentiation. Nonetheless, our limited understanding of
393 their heterogeneity, fate determination, and immunomodulation holds back further MSC
394 applications. It is therefore essential to improve the consistency and efficacy of MSCs. Such
395 enhancement can be achieved using in-vitro preconditioning treatments such as HS (Choudhery,
396 2021). Here we show that the correct application of HS allows for the enhancement of desired MSC
397 characteristics and induction of a wide range of stem cell fates and differentiation pathways.

398

399 **Materials and Methods**

400 **Cell Culture**

401 Bovine mesenchymal stem cells were isolated, cultured and characterized based on generally
402 accepted criteria (Dominici et al., 2006; Uccelli & al., 2008) as we have previously reported (Nir &
403 Ribarski-Chorev et al., 2022; Shimoni et al., 2020). Briefly, umbilical cords of Holstein dairy cows
404 were obtained from abattoirs located in the north of Israel. In the lab, the umbilical cords were
405 digested and plated as previously described in (Toupadakis et al., 2010), followed by expansion in
406 low glucose Dulbecco's Modified Eagle's Medium (Gibco, 31885-023 or Biological Industries (BI),
407 04-001-1A), containing 10% Fetal Bovine Serum (FBS) (BI, 04-001-1A), penicillin-streptomycin
408 solution 1% (BI, 03-031-1B), Glutamine 1% (BI, #03-020-1B) and cryopreserved at different
409 passages using FBS with 10% DMSO (Sigma-Aldrich, W387520). The media was changed every 2-

410 3 days and all cells were cultured in a humidified incubator with a controlled environment of 5%
411 CO2 and a temperature of 37°C, unless mentioned otherwise.

412 **Cell Characterization**

413 Three bovine MSCs lines were used in this study. Two were previously examined and verified (Nir
414 & Ribarski-Chorev et al., 2022; Shimoni et al., 2020) and the third was examined and verified in
415 this study (Supplementary Figure 1 (S1A-S1C)) before subsequent heat shock experiments. One
416 line was used for the RNA-seq experiment, while all three lines were used for RNA-seq validation
417 and further examinations. All the experiments described were done on cells in passages 2-4, and at
418 least 3 biological replicas were used unless specified otherwise.

419 **Cell Death Quantification Using Propidium Iodide (PI)**

420 For quantification of cell death in culture, cells were harvested by trypsinization, washed with PBS,
421 and re-suspended in 10 g/mL PI for 5 min on ice. The percentage of live/dead cells was determined
422 within 1 hour of staining by flow cytometry (CytoFLEX, Beckman Coulter, Indianapolis, IN, USA).
423 10,000 events were collected per sample. At least three biological repeats were used for each
424 treatment. Data analysis was performed using Flow-Jo software.

425 **Heat-shock Induction**

426 MSCs at early passages (P2–P4) were seeded in 6-well plates (Costar, 3516) at different
427 concentrations to allow similar confluence at the end of the experiment, as follows:

Time of treatment	Temperature	# of cells seeded	abbreviation
six hours	37°C	250,000	ShortNT
	40.5°C	250,000	ShortHS
Three days	37°C	42,000	LongNT
	Six hours at 40.5°C, three days recovery at 37°C	72,000	ShortHS_Recovery
	40.5°C	72,000	LongHS

428 The cells were incubated for 24 hours in normal conditions before treatment onset (time 0).

429 **Cell Counting**

430 Following the HS, the cells were washed with Dulbecco's Phosphate Buffered Saline (BI, 02-021-IA)
431 and trypsinized (BI, 03-053-1A). 6µL of trypsinized cells were mixed with 6µL of trypan-blue
432 (Sigma, T8154), loaded into an appropriate slide, and counted using an automated cell counter
433 (TC20, Bio-Rad Laboratories Hercules, CA, USA). Three to five biological repeats were performed.

434 **RNA-sequencing**

435 Total RNA from the heat shocked cells was extracted via PureLink RNA Minikit (Invitrogen,
436 12183018A). RNA concentrations were measured using a NanoDrop ND-1000 spectrophotometer
437 (NanoDrop Technologies) and the quality of extracted RNA was confirmed (RNA integrity number
438 (RIN) > 9) using an Agilent 2100Bioanalyzer before further processing. Library preparation was
439 done using the INCPM mRNA library of the Weizmann Institute, Rehovot. The quality of cDNA
440 libraries was determined using a tape-station. Sequencing was done using Nextseq Illumina in the
441 INCPM of Weizmann Institute, with single-end reads of 75bp. Sequencing was done on 14 samples
442 from the same MSC line as in (Shimoni et al., 2020), and after initial quality analysis one sample
443 was removed and we were left with 13 samples to perform the in-depth analysis: 3 biological
444 replicas for ShortNT, ShortHS and LongHS treatments, and 2 biological replicas for LongNT and
445 ShortHS_Recovery treatments.

446 **Data Analysis**

447 Following sequencing, reads were trimmed using Cutadapt, mapped to genome (Bos_taurus.ARS-
448 UCD1.2) and counted using STAR and HTSeq. Further quality control of alignment sequencing
449 data was done using the Qualimap. Normalization of the counts and differential expression
450 analysis were performed using DESeq2. Hierarchical and K-means clustering as well as data

451 visualizations were performed using R packages. Gene names were taken from the Ensemble
452 BioMart ARS-UCD1.2 dataset. Gene Ontology (GO), KEGG and Reactome pathways enrichment
453 analyses were conducted using both ranked gene list analyses using Gene Set Enrichment Analysis
454 (GSEA) software version 4.1.0 and DEGs list analysis using g:Profiler version
455 e103_eg50_p15_eadf141 and ClueGO v2.5.7 (Cytoscape plug-in) with default parameters. KEGG
456 pathway maps were downloaded from KEGG pathway database. String datasets were used for
457 functional protein association networks. Epigenetic complexes analysis was performed using the
458 EpiFactors Database (Medvedeva et al., 2015) as well GO annotations of the MGI database (Mouse
459 Genome Informatics). The cytokine pathway list was taken from PathCards v5.7.551.0. Bivalent
460 genes enrichment was done by comparing our list to "3,868 bona-fide bivalent genes" in
461 supplementary table No. 1 of (Mas et al., 2018). For detailed information see Supplementary
462 Materials and Methods.

463 **RNA extraction, Reverse transcription, and Real-time PCR**

464 RNA extraction from cells was carried out using GenElute™ Total RNA Purification Kit (Sigma,
465 RNB100-50RXN). RNA was then reverse-transcribed into cDNA using qScriptTM cDNA Synthesis
466 Kit (Quanta-bio, 95047-100). Real-Time PCR (RT-qPCR) reactions were performed using Fast
467 SYBR Green Master Mix (Applied Biosystem, 4385614) in an ABI Step-One Plus Real-Time PCR
468 system. All primers were verified by standard curve evaluation and are shown in Supplementary
469 Table S1. Primers for expression analysis were designed on exon-exon junctions and a -RT control
470 was performed each time. Relative mRNA fold change was calculated with the ΔΔCT method,
471 using 1-2 control genes (PSMB2 and RPS9) as reference.

Statistical Analysis

GraphPad Prism (La Jolla, CA, United States) was used for statistical analysis and visualization of RT-qPCR. $p < 0.05$ was considered statistically significant. For enrichment analysis hypergeometric p-value was calculated using The Graeber Lab online calculator 2009 © (https://systems.crump.ucla.edu/hypergeometric/). See Supplementary Materials and Methods for more detailed information.

Availability of data and materials

The datasets supporting the conclusions of this article are available in the GEO repository, GSE214467 study at: https://www.ncbi.nlm.nih.gov/geo/query/acc.cgi?acc=GSE214467

Some datasets supporting the conclusions of this article are included within the article additional files.

Acknowledgments

We are grateful to all the members of the Schlesinger lab for their ideas and support; Prof. Z. Roth for scientific discussion, encouragement and support; Joseph Kippen for critical reading and reviewing; the Weizmann Institute Next Generation Sequencing Facility, for sequencing support; The authors also thank Dr. S. Shainin and Mr. S. Yaakobi from the Volcani Center for help with obtaining the umbilical cords.

Authors contributions

IRH: conception and design, designing and performed the experiments, bioinformatics analysis and data interpretation, and manuscript writing. GS: validation of MSC lines by flow and RT-qPCR. CS: support with MSC extraction and culturing. SS: conception and design, assembly of data and data analysis, manuscript writing. The authors read and approved the final manuscript.

Competing interests

The authors declare that they have no competing interests.

Funding

This work was funded by a US-Israel Binational Agricultural Research and Development Fund research project #IS-5067-18 and the Israeli Ministry of Agriculture and Rural Development grant #12- 04-0014.

502 **Ethics approval and consent to participate**

503 The procedures of isolated UC-MSCs were conducted abiding by the Institutional Animal Care and
504 Use Committee of the Israel Ministry of Agriculture and Rural Development, permit #11380.

505 **List of abbreviations**

506 MSCs:

507 Mesenchymal stem cells

508 bUC-MSCs:

509 Bovine umbilical cord-derived mesenchymal stem cells

510 ER:

511 endoplasmic reticulum

512 FBS:

513 Fetal Bovine Serum

514 RNA-seq:

515 RNA sequencing

516 RT-qPCR:

517 Reverse transcriptase- quantitative polymerase chain reaction

518 HS:

519 Heat shock

520 NT:

521 Normothermic

522 DEGs:

523 Differentially expressed genes

524 GSEA:

525 Gene set enrichment analysis

526 GO:

527 Gene ontology

528 ECM:

529 Extracellular matrix

530 PcG:

531 Polycomb group

532 MLL:

533 Mixed lineage leukemia

534 H3K4me3:

535 The trimethylation of histone H3 Lys 4

536 ILs:

537 Interleukins

538

539 **References**

540 Abdal Dayem, A., Lee, S., Y. Choi, H., & Cho, S. G. (2018). The Impact of Adhesion Molecules on the
541 In Vitro Culture and Differentiation of Stem Cells. *Biotechnology Journal*, *13*(2), 1700575.
542 https://doi.org/10.1002/BIOT.201700575

543 Agarwal, A., Virk, G., Ong, C., & Plessis, S. S. du. (2014). Effect of Oxidative Stress on Male
544 Reproduction. *The World Journal of Men's Health*, *32*(1), 1.
545 https://doi.org/10.5534/WJMH.2014.32.1.1

546 Antonioli, E., Torres, N., Ferretti, M., de Azevedo Piccinato, C., & Sertie, A. L. (2019). Individual
547 response to mTOR inhibition in delaying replicative senescence of mesenchymal stromal cells.
548 *PLoS ONE*, *14*(1). https://doi.org/10.1371/JOURNAL.PONE.0204784

549 Asseng, S., Spänkuch, D., Hernandez-Ochoa, I. M., & Laporta, J. (2021). The upper temperature
550 thresholds of life. *The Lancet Planetary Health*, *5*(6), e378–e385.
551 https://doi.org/10.1016/S2542-5196(21)00079-6

552 Bagath, M., Krishnan, G., Devaraj, C., Rashamol, V. P., Pragna, P., Lees, A. M., & Sejian, V. (2019).
553 The impact of heat stress on the immune system in dairy cattle: A review. *Research in*
554 *Veterinary Science*, *126*, 94–102. https://doi.org/10.1016/J.RVSC.2019.08.011

555 Chen, S., Wang, J., Peng, D., Li, G., Chen, J., & Gu, X. (2018). Exposure to heat-stress environment
556 affects the physiology, circulation levels of cytokines, and microbiome in dairy cows. *Scientific*
557 *Reports 2018 8:1*, *8*(1), 1–11. https://doi.org/10.1038/s41598-018-32886-1

558 Choudhery, M. S. (2021). Strategies to improve regenerative potential of mesenchymal stem cells.
559 *World Journal of Stem Cells*, *13*(12), 1845. https://doi.org/10.4252/WJSC.V13.I12.1845

560 Collier, R. J., Stiening, C. M., Pollard, B. C., VanBaale, M. J., Baumgard, L. H., Gentry, P. C., &
561 Coussens, P. M. (2006). Use of gene expression microarrays for evaluating environmental
562 stress tolerance at the cellular level in cattle. *Journal of Animal Science*, *84*(suppl_13), E1–E13.
563 https://doi.org/10.2527/2006.8413_SUPPLE1X

564 Dado-Senn, B., Laporta, J., & Dahl, G. E. (2020). Carry over effects of late-gestational heat stress on
565 dairy cattle progeny. *Theriogenology*, *154*, 17–23.
566 https://doi.org/10.1016/J.THERIOGENOLOGY.2020.05.012

567 Dalton, S., & Coverdell, P. D. (2015). Linking the cell cycle to cell fate decisions. *Trends in Cell*
568 *Biology*, *25*(10), 592. https://doi.org/10.1016/J.TCB.2015.07.007

569 de Barros, F. R. O., & Paula-Lopes, F. F. (2018). Cellular and epigenetic changes induced by heat
570 stress in bovine preimplantation embryos. *Molecular Reproduction and Development*, *85*(11),
571 810–820. https://doi.org/10.1002/MRD.23040

572 Dominici, M., Le Blanc, K., Mueller, I., Slaper-Cortenbach, I., Marini, F. C., Krause, D. S., Deans, R.
573 J., Keating, A., Prockop, D. J., & Horwitz, E. M. (2006). Minimal criteria for defining
574 multipotent mesenchymal stromal cells. The International Society for Cellular Therapy
575 position statement. *Cytotherapy*, *8*(4), 315–317. https://doi.org/10.1080/14653240600855905

576 Dou, J., Cánovas, A., Brito, L. F., Yu, Y., Schenkel, F. S., & Wang, Y. (2021). Comprehensive RNA-
577 Seq Profiling Reveals Temporal and Tissue-Specific Changes in Gene Expression in Sprague–
578 Dawley Rats as Response to Heat Stress Challenges. *Frontiers in Genetics*, *12*, 420.
579 https://doi.org/10.3389/FGENE.2021.651979/BIBTEX

580 Ermolaeva, M., Neri, F., Ori, A., & Rudolph, K. L. (2018). Cellular and epigenetic drivers of stem cell
581 ageing. *Nature Reviews Molecular Cell Biology 2018 19:9*, *19*(9), 594–610.
582 https://doi.org/10.1038/s41580-018-0020-3

583 Fang, H., Kang, L., Abbas, Z., Hu, L., Chen, Y., Tan, X., Wang, Y., & Xu, Q. (2021). Identification of
584 key Genes and Pathways Associated With Thermal Stress in Peripheral Blood Mononuclear
585 Cells of Holstein Dairy Cattle. *Frontiers in Genetics*, *12*, 910.
586 https://doi.org/10.3389/FGENE.2021.662080/BIBTEX

587 Gao, S. T., Ma, L., Zhou, Z., Zhou, Z. K., Baumgard, L. H., Jiang, D., Bionaz, M., & Bu, D. P. (2019).
588 Heat stress negatively affects the transcriptome related to overall metabolism and milk
589 protein synthesis in mammary tissue of midlactating dairy cows. *Physiological Genomics*,
590 *51*(8), 400–409.
591 https://doi.org/10.1152/PHYSIOLGENOMICS.00039.2019/ASSET/IMAGES/LARGE/ZH70091
592 943690006.JPEG

593 Garner, J. B., Chamberlain, A. J., Vander Jagt, C., Nguyen, T. T. T., Mason, B. A., Marett, L. C.,
594 Leury, B. J., Wales, W. J., & Hayes, B. J. (2020). Gene expression of the heat stress response in
595 bovine peripheral white blood cells and milk somatic cells in vivo. *Scientific Reports 2022*
596 *10:1*, *10*(1), 1–12. https://doi.org/10.1038/s41598-020-75438-2

597 Harikumar, A., & Meshorer, E. (2015). "Histones and Chromatin" Review series: Chromatin
598 remodeling and bivalent histone modifications in embryonic stem cells. *EMBO Reports*,
599 *16*(12), 1609. https://doi.org/10.15252/EMBR.201541011

600 Hass, R., Kasper, C., Böhm, S., & Jacobs, R. (2011). Different populations and sources of human
601 mesenchymal stem cells (MSC): A comparison of adult and neonatal tissue-derived MSC. *Cell*
602 *Communication and Signaling : CCS*, *9*(1), 12. https://doi.org/10.1186/1478-811X-9-12

603 Isik, B., Thaler, R., Goksu, B. B., Conley, S. M., Al-Khafaji, H., Mohan, A., Afarideh, M., Abumoawad,
604 A. M., Zhu, X. Y., Krier, J. D., Saadiq, I. M., Tang, H., Eirin, A., Hickson, L. T. J., van Wijnen, A.
605 J., Textor, S. C., Lerman, L. O., & Herrmann, S. M. (2021). Hypoxic preconditioning induces
606 epigenetic changes and modifies swine mesenchymal stem cell angiogenesis and senescence
607 in experimental atherosclerotic renal artery stenosis. *Stem Cell Research and Therapy*, *12*(1),
608 1–13. https://doi.org/10.1186/S13287-021-02310-Z

609 Johnson, S. C., Rabinovitch, P. S., & Kaeberlein, M. (2013). mTOR is a key modulator of ageing and

610 age-related disease. *Nature*, *493*(7432), 338. https://doi.org/10.1038/NATURE11861

611 Kawano, K., Sakaguchi, K., Madalitso, C., Ninpetch, N., Kobayashi, S., Furukawa, E., Yanagawa, Y.,
612 & Katagiri, S. (2022). Effect of heat exposure on the growth and developmental competence
613 of bovine oocytes derived from early antral follicles. *Scientific Reports 2022 12:1*, *12*(1), 1–14.
614 https://doi.org/10.1038/s41598-022-12785-2

615 Key, N., Sneeringer, S., & Marquardt, D. (2014). Climate Change, Heat Stress, and U.S. Dairy
616 Production. *SSRN Electronic Journal*, *175*. https://doi.org/10.2139/ssrn.2506668

617 Khalid, A. B., Pence, J., Suthon, S., Lin, J., Miranda-Carboni, G. A., & Krum, S. A. (2021). GATA4
618 regulates mesenchymal stem cells via direct transcriptional regulation of the WNT
619 signalosome. *Bone*, *144*, 115819. https://doi.org/10.1016/J.BONE.2020.115819

620 Khan, A., Dou, J., Wang, Y., Jiang, X., Khan, M. Z., Luo, H., Usman, T., & Zhu, H. (2020). Evaluation
621 of heat stress effects on cellular and transcriptional adaptation of bovine granulosa cells.
622 *Journal of Animal Science and Biotechnology*, *11*(1). https://doi.org/10.1186/S40104-019-
623 0408-8

624 Kitagawa, Y., Suzuki, K., Yoneda, A., & Watanabe, T. (2004). Effects of oxygen concentration and
625 antioxidants on the in vitro developmental ability, production of reactive oxygen species
626 (ROS), and DNA fragmentation in porcine embryos. *Theriogenology*, *62*(7), 1186–1197.
627 https://doi.org/10.1016/J.THERIOGENOLOGY.2004.01.011

628 Kou, M., Huang, L., Yang, J., Chiang, Z., Chen, S., Liu, J., Guo, L., Zhang, X., Zhou, X., Xu, X., Yan,
629 X., Wang, Y., Zhang, J., Xu, A., Tse, H., & Lian, Q. (2022). Mesenchymal stem cell-derived
630 extracellular vesicles for immunomodulation and regeneration: a next generation therapeutic
631 tool? *Cell Death & Disease 2022 13:7*, *13*(7), 1–16. https://doi.org/10.1038/s41419-022-05034-
632 x

633 Kuroda, Y., & Dezawa, M. (2014). Mesenchymal stem cells and their subpopulation, pluripotent
634 muse cells, in basic research and regenerative medicine. *Anatomical Record*, *297*(1), 98–110.
635 https://doi.org/10.1002/ar.22798

636 Li, J., Labbadia, J., & Morimoto, R. I. (2017). Rethinking HSF1 in Stress, Development, and
637 Organismal Health. *Trends in Cell Biology*, *27*(12), 895–905.
638 https://doi.org/10.1016/J.TCB.2017.08.002

639 Madrigal, M., Rao, K. S., & Riordan, N. H. (2014). A review of therapeutic effects of mesenchymal
640 stem cell secretions and induction of secretory modification by different culture methods.
641 *Journal of Translational Medicine*, *12*(1), 1–14. https://doi.org/10.1186/s12967-014-0260-8

642 Mas, G., Blanco, E., Ballaré, C., Sansó, M., Spill, Y. G., Hu, D., Aoi, Y., Le Dily, F., Shilatifard, A.,
643 Marti-Renom, M. A., & Di Croce, L. (2018). Promoter bivalency favors an open chromatin
644 architecture in embryonic stem cells. *Nature Genetics 2018 50:10*, *50*(10), 1452–1462.
645 https://doi.org/10.1038/s41588-018-0218-5

646 Medvedeva, Y. A., Lennartsson, A., Ehsani, R., Kulakovskiy, I. V., Vorontsov, I. E., Panahandeh, P.,
647 Khimulya, G., Kasukawa, T., & Drabløs, F. (2015). EpiFactors: a comprehensive database of
648 human epigenetic factors andcomplexes. *Database: The Journal of Biological Databases and*
649 *Curation*, *2015*. https://doi.org/10.1093/DATABASE/BAV067

650 Moise, S., Byrne, J. M., El Haj, A. J., & Telling, N. D. (2018). The potential of magnetic hyperthermia
651 for triggering the differentiation of cancer cells. *Nanoscale*, *10*(44), 20519–20525.
652 https://doi.org/10.1039/C8NR05946B

653 Naaldijk, Y., Johnson, A. A., Ishak, S., Meisel, H. J., Hohaus, C., & Stolzing, A. (2015). Migrational
654 changes of mesenchymal stem cells in response to cytokines, growth factors, hypoxia, and
655 aging. *Experimental Cell Research*, *338*(1), 97–104.
656 https://doi.org/10.1016/J.YEXCR.2015.08.019

657 Nir & Ribarski-Chorev, D., Ribarski-Chorev, I., Shimoni, C., Strauss, C., Frank, J., & Schlesinger, S.
658 (2022). Antioxidants Attenuate Heat Shock Induced Premature Senescence of Bovine
659 Mesenchymal Stem Cells. *International Journal of Molecular Sciences*, *23*(10), 5750.
660 https://doi.org/10.3390/ijms23105750

661 Noer, A., Lindeman, L. C., & Collas, P. (2009). Histone H3 modifications associated with
662 differentiation and long-term culture of mesenchymal adipose stem cells. *Stem Cells and*
663 *Development*, *18*(5), 725–736. https://doi.org/10.1089/scd.2008.0189

664 Nowakowski, A., Drela, K., Rozycka, J., Janowski, M., & Lukomska, B. (2016). Engineered
665 Mesenchymal Stem Cells as an Anti-Cancer Trojan Horse. *Stem Cells and Development*,
666 *25*(20), 1513–1531. https://doi.org/10.1089/scd.2016.0120

667 Olde Riekerink, R. G. M., Barkema, H. W., & Stryhn, H. (2007). The Effect of Season on Somatic
668 Cell Count and the Incidence of Clinical Mastitis. *Journal of Dairy Science*, *90*(4), 1704–1715.
669 https://doi.org/10.3168/JDS.2006-567

670 Peters, A., Nawrot, T. S., & Baccarelli, A. A. (2021). Hallmarks of environmental insults. *Cell*,
671 *184*(6), 1455–1468. https://doi.org/10.1016/J.CELL.2021.01.043

672 Phinney, D. G., & Pittenger, M. F. (2017). Concise Review: MSC-Derived Exosomes for Cell-Free
673 Therapy. *STEM CELLS*, *35*(4), 851–858. https://doi.org/10.1002/STEM.2575

674 Pittenger, M. F., Mackay, A. M., Beck, S. C., Jaiswal, R. K., Douglas, R., Mosca, J. D., Moorman, M.
675 A., Simonetti, D. W., Craig, S., & Marshak, D. R. (1999). Multilineage potential of adult human
676 mesenchymal stem cells. *Science*, *284*(5411), 143–147.
677 https://doi.org/10.1126/SCIENCE.284.5411.143/SUPPL_FILE/983855S5_THUMB.GIF

678 Richter, K., Haslbeck, M., & Buchner, J. (2010). The Heat Shock Response: Life on the Verge of
679 Death. *Molecular Cell*, *40*(2), 253–266.
680 https://doi.org/10.1016/J.MOLCEL.2010.10.006/ATTACHMENT/BFF2FC30-41D1-4EE0-9FE1-
681 1D8B605F6F20/MMC1.PDF

682 Roth, Z. (2017). Effect of Heat Stress on Reproduction in Dairy Cows: Insights into the Cellular and
683 Molecular Responses of the Oocyte. *Http://Dx.Doi.Org/10.1146/Annurev-Animal-022516-*
684 *022849*, *5*, 151–170. https://doi.org/10.1146/ANNUREV-ANIMAL-022516-022849

685 Roth, Z. (2020). Reproductive physiology and endocrinology responses of cows exposed to
686 environmental heat stress - Experiences from the past and lessons for the present.
687 *Theriogenology*, *155*, 150–156. https://doi.org/10.1016/J.THERIOGENOLOGY.2020.05.040

688 Sammad, A., Luo, H., Hu, L., Zhu, H., & Wang, Y. (2022). Transcriptome Reveals Granulosa Cells
689 Coping through Redox, Inflammatory and Metabolic Mechanisms under Acute Heat Stress.

690 *Cells*, *11*(9). https://doi.org/10.3390/CELLS11091443/S1

691 Saxton, R. A., & Sabatini, D. M. (2017). mTOR Signaling in Growth, Metabolism, and Disease. *Cell*,
692 *168*(6), 960–976. https://doi.org/10.1016/J.CELL.2017.02.004

693 Schultz, M. B., & Sinclair, D. A. (2016). When stem cells grow old: phenotypes and mechanisms of
694 stem cell aging. *Development*, *143*(1), 3–14. https://doi.org/10.1242/DEV.130633

695 Sharma, S., & Bhonde, R. (2020). Genetic and epigenetic stability of stem cells: Epigenetic
696 modifiers modulate the fate of mesenchymal stem cells. *Genomics*, *112*(5), 3615–3623.
697 https://doi.org/10.1016/J.YGENO.2020.04.022

698 Shimoni, C., Goldstein, M., Ribarski-Chorev, I., Schauten, I., Nir, D., Strauss, C., & Schlesinger, S.
699 (2020). Heat Shock Alters Mesenchymal Stem Cell Identity and Induces Premature
700 Senescence. *Frontiers in Cell and Developmental Biology*, *8*(September), 1–15.
701 https://doi.org/10.3389/fcell.2020.565970

702 Stopp, S., Bornhäuser, M., Ugarte, F., Wobus, M., Kuhn, M., Brenner, S., & Thieme, S. (2013).
703 Expression of the melanoma cell adhesion molecule in human mesenchymal stromal cells
704 regulates proliferation, differentiation, and maintenance of hematopoietic stem and
705 progenitor cells. *Haematologica*, *98*(4), 505–513.
706 https://doi.org/10.3324/HAEMATOL.2012.065201

707 Su, K. H., & Dai, C. (2017). mTORC1 senses stresses: Coupling stress to proteostasis. *BioEssays :*
708 *News and Reviews in Molecular, Cellular and Developmental Biology*, *39*(5).
709 https://doi.org/10.1002/BIES.201600268

710 Toupadakis, C. A., Wong, A., Genetos, D. C., Cheung, W. K., Borjesson, D. L., Ferraro, G. L.,
711 Galuppo, L. D., Leach, J. K., Owens, S. D., & Yellowley, C. E. (2010). Comparison of the
712 osteogenic potential of equine mesenchymal stem cells from bone marrow, adipose tissue,
713 umbilical cord blood, and umbilical cord tissue. *American Journal of Veterinary Research*,
714 *71*(10), 1237–1245. https://doi.org/10.2460/AJVR.71.10.1237

715 Uccelli, A., & al., et. (2008). Mesenchymal stem cells in health and disease. *Nat. Rev. Immunol.*, *8*,
716 726–736.

717 Uccelli, A., Moretta, L., & Pistoia, V. (2008). Mesenchymal stem cells in health and disease. *Nat Rev*
718 *Immunol*, *8*(9), 726–736. https://doi.org/10.1038/nri2395

719 van Velthoven, C. T. J., & Rando, T. A. (2019). Stem Cell Quiescence: Dynamism, Restraint, and
720 Cellular Idling. *Cell Stem Cell*, *24*(2), 213. https://doi.org/10.1016/J.STEM.2019.01.001

721 Xue, Y., & Acar, M. (2018). Mechanisms for the epigenetic inheritance of stress response in single
722 cells. *Current Genetics*, *64*(6), 1221. https://doi.org/10.1007/S00294-018-0849-1

723 Yue, S., Wang, Z., Wang, L., Peng, Q., & Xue, B. (2020). Transcriptome Functional Analysis of
724 Mammary Gland of Cows in Heat Stress and Thermoneutral Condition. *Animals : An Open*
725 *Access Journal from MDPI*, *10*(6), 1–18. https://doi.org/10.3390/ANI10061015

726 Zhang, Y., Ling, L., Ajay D/O Ajayakumar, A., Eio, Y. M., van Wijnen, A. J., Nurcombe, V., & Cool, S.
727 M. (2022). FGFR2 accommodates osteogenic cell fate determination in human mesenchymal
728 stem cells. *Gene*, *818*, 146199. https://doi.org/10.1016/J.GENE.2022.146199

731 **Figure legends:**

732 **Figure 1**: **Transcriptome changes in response to heat shock**. **(A)** A schematic timeline showing
733 the HS treatments from which RNA-Seq libraries were prepared. MSCs were plated and 24h later
734 exposed to heat shock (HS, 40.5°C) for: 6h (ShortHS), 6h + 3 days recovery at 37°C
735 (ShortHS_Recovery), 72h (LongHS), followed by collection for RNA extraction. Control cells were
736 parallelly plated and maintained in normal temperature (NT, 37°C). Each treatment has colour
737 code which will be used throughout the article: **ShortNT (red), ShortHS (green), LongNT**
738 **(olive), ShortHS_Recovery (blue), LongHS (purple)**. **(B)** Scatter plot for principal component
739 analysis of global gene expression (RNA-seq) demonstrates clear separation of gene transcripts
740 between groups. **(C)** Number of differentially expressed genes (DEGs) with padj ≤0.05 and
741 log2(FC)≥1 that change between the treatment groups. **(D)** K-means clustering of 3667 DEGs.

742 **Figure 2: Downregulation of cell cycle and immune response genes while developmental**
743 **pathways genes are induced following long heat shock. (A)** Illustration of long heat shock
744 treatment. **(B)** Cells after LongHS get enlarged and flattened. Bright field x4 (up) and x10 (down).
745 Arrows point to stress granules. **(C)** Results of GSEA Hallmark analysis showing enriched gene
746 sets (FDR q-val < 25% and p-val < 0.05). A positive normalized enrichment score (NES) values,
747 mark in red, indicates upregulation in the LongHS phenotype. **(D)** Differentiation pathways
748 significantly upregulated in LongHS vs. LongNT as per g:Profiler analysis. Plot was generated
749 using GOplot R package. **(E)** Upregulated histone modifications and PcG complex following
750 LongHS as per GO analysis with GSEA. **(F)** KEGGs significantly upregulated in differentially
751 expressed genes of LongHS vs LongNT using ClueGo. Colors represented p-value: light red 0.05,
752 red 0.01, brown 0.001. The node size represents the term enrichment significance.

753 **Figure 3: Induced stress response and reduced cellular functions following short heat shock.**
754 **(A)** Illustration of short heat shock treatment. **(B-E)** Gene set enrichment analysis (GSEA) results
755 of 40.5c6h vs. control comparison. RNA-Seq was performed on samples collected after 6 hours at
756 40.5c compared to cells cultured in 37c (control). **(B)** Heat map of the top 30 marker genes
757 upregulated and downregulated in short heat stress. Expression values are represented as colors
758 and range from red (high expression), pink (moderate), light blue (low) to dark blue (lowest
759 expression). **(C)** Results of GSEA Hallmark analysis showing enriched gene sets (FDR q-val < 25%
760 and p-val < 0.05). A positive normalized enrichment score (NES) values, marked in red, indicate

761 enrichment in the 40.5c6h phenotype. **(D)** Upregulated GSEA biological processes significantly
762 enriched (FDR q-val < 0.25 and p-val< 0.01) in the comparison of ShortHS vs. ShortNT, ordered
763 by the increasing NES (dark color is the most enriched). Due to high number of GOs, the GOs with
764 similar process were combined under one general phrase, which is represented by one part of the
765 pie chart (Supplementary Table S4). The number defines average normalized enrichment score.
766 **(E)** Downregulated GSEA biological processes significantly decreased (FDR q-val < 0.25, p-val <
767 0.01) in the comparison of ShortHS vs. ShortNT, ordered by the increasing NES. **(F)** Functional
768 enrichment analysis of the upregulated (red) and downregulated (blue) differentially expressed
769 genes (DEGs) between ShortHS and ShortNT cells using g:Profiler.

770 **Figure 4: Transient upregulation of chromatin modifiers after short heat shock and stable**
771 **activation of lineage commitment genes, maintained even after three days recovery. (A)**
772 Illustration of ShortHS_Recovery vs ShortHS treatment. **(B)** Heat map of genes differentially
773 expressed (padj < 0.05) between ShortHS and ShortNT. **(C)** Biological processes enriched in
774 cluster 2 (pink) **(D)** Biological processes enriched in cluster 3 (blue) **(E)** Population doubling time
775 for prolonged treated groups. **(F)** Biological processes enriched in cluster 4 (purple) **(G)** MLL
776 (GO:0044665, GO:0044666), HAT (GO:0000123) and HMT (GO:0035097) are upregulated
777 following ShortHS but return to normal/downregulated during recovery period **(H)** Bivalent genes
778 are upregulated following ShortHS and remain in this state even after recovery period.

779 **Figure 5: Cell cycle and metabolism are commonly reduced following all heat shock**
780 **protocols, while other processes related to key characteristics of MSC are differently**
781 **regulated. (A)** Venn diagram of upregulated genes (padj < 0.05) between the treatment groups.
782 **(B)** Venn diagram of downregulated genes (padj < 0.05) between the treatment groups. **(C)** Heat
783 shock common hallmarks and their enrichment score. Above hyphenated line are hallmarks
784 common to all 3 HS groups. **(D)** Cell cycle related biological processes, effected by HS, and their
785 enrichment score. N00455: CDC25-Cell cycle G2/M (KEGG pathway), GO:0007049: Cell cycle
786 (MGI database), R-BTA-69002 – DNA Replication Pre-Initiation (Reactome). **(E)** Enrichment of
787 biological processed related to development effected by HS. GO:0060070: Canonical WNT
788 signalling, GO 0048863: Stem cell differentiation, GO:0048468: Cell development, GO:0009888:
789 Tissue development, GO:0007492: Endoderm development. GO:0007498: Mesoderm
790 development, GO:0048762: mesenchymal cell differentiation. **(F)** Enrichment of biological

791 processed related to immune system effected by HS. GO:0002526: Acute Inflammatory response,
792 GO:1905517: Macrophage migration, GO:0032635: IL-6 production, Cytokine pathway list was
793 taken from PathCards v5.7.551.0. **(G)** Cytokine pathways genes that are differentially expressed in
794 LongHS vs. LongNT.

795

796 **Supplementary figure legends**

797 **Supplementary Figure 1**: **Characterization of the bUC-MSC line used for RNA-seq validation.**
798 (A) Expression of positive (cd29, cd44, cd 90) and negative (cd45) MSC markers normalized to
799 RPS9. (B) Population doubling time, 3-4 biological replicas at each time point. (C) MSCs
800 differentiate to chondrocytes (Alcian blue staining), osteoblasts (Alizarin red staining) and
801 adipocytes (BODIPY™ 493/503 and DAPI staining). Chondrocyte and osteoblast staining was
802 observed using EVOS® FL Auto microscope scale bar 100m. Adipocyte staining was observed
803 using a fluorescent microscope, scale bar 50m. (D) PI staining for live/dead cells after all HS
804 treatments (E) Positive and negative markers of MSC, normalized to RSP9 housekeeping gene,
805 after all HS treatments

806 **Supplementary Figure 2**: **RNA-seq quality**. Bio detection histogram (Qualimap application)
807 showing which kind of features are being detected in control **(A)** vs. HS **(B)** groups, similar
808 distribution was seen in all samples. The x-axis shows all the groups included in the annotations
809 file. The gray bars are the percentage of features of each group within the reference genome. The
810 striped color bars are the percentages of features of each group detected in the sample with
811 regards to the reference. The solid color bars are the percentages that each group represents in the
812 total detected features in the sample. **(C)** Hierarchical clustering of the samples presents clustering
813 by treatments and by the time the cells were in the cutler (culturing effect). **(D)** Validation of RNA-
814 seq by RT-qPCR. Raw read counts were used for sequencing data plots. **(E)** The direction of DEGs
815 regulation per treatment, shows more genes are downregulated during heat shock than
816 upregulated.

817 **Supplementary Figure 3: Transcriptional changes in differentially expressed genes of MSC**
818 **following heat shock. (A)** K-means clustering of 3667 DEGs, with main biological processes in
819 each cluster. **(B-H).** Focusing on DEGs enrichment for each treatment pair. Each graph: In the top

820 left there is a barplot for the number of DEGs in each cluster. The main graph is a scatterplot of the
821 RNA-seq enrichment. Axes colours match treatment colour coding [ShortNT (red), ShortHS
822 (green), LongNT (olive), ShortHS_Recovery (blue), LongHS (purple)]. Each axis represents
823 upregulated DEGs of specific treatment as specified on the axes. DEGs coloring matches the color
824 code of clusters and biological processes in figure A, right side. Non-differential genes are gray.

825 **Supplementary Figure 4: LongHS halts cell cycle and promotes cell developmental fate. (A)**
826 Cell cycle arrest during LongHS (KEGG Pathway bta041100). Upregulated (pink) and down
827 (yellow) DEGs (padj <0.05 and log2(FC) >1) of LongHS treatment are marked. On right side, RT-
828 PCR validation of cell cycle genes, normalized to PSMB. (B) Upregulated DEGs marked in red of
829 adhesion molecules (KEGG map bta04514) following LongHS. (C) Upregulated DEGs marked in
830 red of axon guidance (KEGG map bta04360) following LongHS.

831 **Supplementary Figure 5: ShortHS halts DNA replication. (A)** Genome viewer (IGV) screenshot
832 of genes that become significantly up-regulated following HS treatments. FOXF1-transcription
833 factor associated with cell differentiation; AHSA2 - activator of HSP90. **(B)** DNA replication is
834 downregulated during ShortHS (KEGG map bta03030). Downregulated (blue) DEGs (padj <0.05
835 and log2(FC) >1) are marked.

836 **Supplementary Figure 6: Upregulated bivalent genes following ShortHS that maintain**
837 **direction of regulation during recovery period.** Biological process (BPs) enriched for bivalent
838 genes found in Cluster 2 of Figure 4B, lowly expressed genes in the control sample that were
839 upregulated after the short HS and remained active during recovery. (BP's term size used in
840 g:Profiler was between 5-1000; Figure prepared using GOChord plot in RStudio). On right is BPs
841 with color coding as per the legend. From left are genes common to at least 4 BPs, arranged by
842 log2 Fold Change.

843 **Supplementary Figure 7: Cell functions modified by heat shock. (A)** Hallmarks affected by
844 specific heat shock treatments. ShortHS has no specific process, only ShortHS_Recovery, and
845 LongHS groups. **(B)** All genes with padj<0.05 and no culturing effect that are affected by HS
846 treatments in the cell cycle (KEGG Pathway bta041100). Blue and red, downregulated and
847 upregulated genes accordingly.

848 **Supplementary Figure 8: Culturing effects on MSC transcriptome**. **(A)** Illustration of control
849 groups examined. **(B)** Hallmark gene sets enrichment of LongNT vs. ShortNT. Results of GSEA
850 Hallmark analysis show enriched gene sets (FDR q-value < 25% and p-val < 0.05). A positive
851 normalized enrichment score (NES) values, marked in red, indicate enrichment in the LongNT
852 phenotype. **(C)**. Circadian clock genes changed during normal cell growth (STRING network).
853 Upregulated and downregulated following three days culturing are marked in red and blue
854 accordingly.

855

856 **Tables and their legends**

857 Supplementary Table 1: List of all bovine primers used in this study for gene expression analysis
858 by RT-qPCR
859 Supplementary Table 2: Samples used for RNA-seq
860 Supplementary Table 3: Culturing conditions of the samples used in heat shock experiments
861 Supplementary Table S4: Biological process upregulated in ShortHS - term convergence
862 Supplementary Table 5: List of GSEA GOBPs related to immune system and downregulated in
863 LongHS
864 Supplementary Table 6: RNA-seq data analysis using DESeq
865 Supplementary Table 7: HS specific and common genes with no culturing effect
866

867 **Supplementary Materials and Methods**

868 **RNA-seq data processing**

869 Following sequencing, reads were trimmed for adaptors and poly A using Cutadapt, checked for
870 quality by FastQC, mapped to genome (Bos_taurus.ARS-UCD1.2) and counted using STAR and
871 HTSeq accordingly. Further quality control of alignment sequencing data was done using
872 Integrative Genomics Viewer (IVG) and Qualimap application (Okonechnikov et al., 2016;
873 Robinson et al., 2011). Normalization of the counts and differential expression analysis were
874 performed using DESeq2 package in RStudio (RStudio Team, 2022). Total of 27,607 genes were
875 sequenced. Genes with less then 5 counts in total per all treatments were removed, and we left
876 with 16,595 genes for further downstream analyses (Supplementary Table S6). PCA, hierarchical
877 and K-means clustering as well as other data visualizations, were performed using Rstudio.

878 **Functional enrichment analysis for immediate HS treatments (ShortHS & LongHS)**

879 To get a comprehensive understanding of all the changes that occurred following the HS, we
880 delved into the functional enrichment analysis using GSEA, g:Profiler and ClueGo tools, as
881 recommended by Reimand et. al. (Bindea et al., 2009; Reimand et al., 2019; Zielniok et al., 2021).
882 Initially, genes with adjusted p-value (padj) < 0.05 and log2 Fold Change log2(FC) >1 were defined
883 as DEGs. Gene Ontology (GO), Kyoto Encyclopedia of Genes and Genomes (KEGG) and Reactome
884 pathways analysis was performed on DEGs using g:Profiler version e103_eg50_p15_eadf141 and
885 ClueGO v2.5.7 (Cytoscape plug-in). In both tools default parameters with pv < 0.05 and bovine

genome ARS-UCD1.2 were used. Analysis was performed for annotated genes only. In g:Profiler the analysis results were then filtered to display only terms sized between 5 and 350 genes, unless specified otherwise. DEG analysis was used in Figures 1-3 and supplementary figure S3.

Afterwards we continued the enrichment analysis using Gene Set Enrichment Analysis (GSEA) software. Since this is a human database, bovine gene names matching our gene id were taken from Ensemble BioMart ARS-UCD1.2. dataset and cross referenced with human orthologs from bioDBnet (biological DataBase network). Into GSEA, we entered the ranked list of all available genes from DESeq analysis (16,595) who have human ortholog (14,205). The enriched Hallmarks and GO pathways with a false discovery rate (FDR) less than 25% and p nominal value of less than 0.05 were considered significantly meaningful. Settings used; 1000 permutations, collapse dataset to gene symbols - false, permutation type - gene set, default parameters in basic and advanced fields. GSEA analysis was used in Figures 2-3,5C and supplementary figures S7-8.

Functional enrichment analysis for long term effects of HS

At the end, we wanted to check for any long-term effects of short HS and to compare between different HS groups. To this end, we re-analysed the data.

First, to eliminate culturing effect and focus on genes influenced by heat stress alone, the genes that changed between controls groups (Short and Long NT) were removed from the analysis. For this, all 16,595 sequenced genes were clustered, and 2 clusters (cluster 1 and 8 in Figure S9) were removed from gene list. Therefore 11679 genes left for further analysis. From 11,679 genes only 3,993 genes are with padj < 0.05 between ShortNT control and HS as shown in figure 4B. These 3,993 were used for functional enrichment analysis of long-term effect of HS (Figure 4), using g: Profiler e106_eg53_p16_65fcd97 with same parameters as stated previously.

Figure S9: K-means clustering of 16595 genes from the sequencing. Cluster 1 and 8 were removed from gene list, Total of 11679 out of 16595 genes left for further analysis.

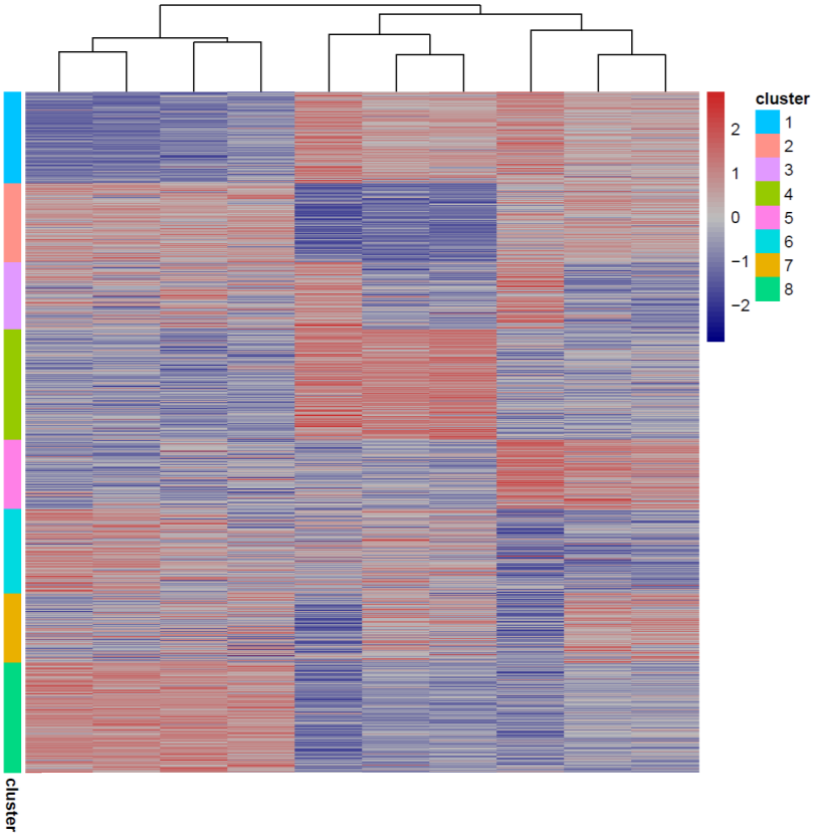

Since following ShortHS there was upregulation of many epigenetic changes (Figure 4F), we wanted to check if there's any enrichment of specific epigenetic complexes. For this analysis was used complexes gene list from EpiFactors Database (Medvedeva et al., 2015) as well GO annotations of MGI database (Mouse Genome Informatics): MLL (GO:0044665, GO:0044666), HAT (GO:0000123) and HMT (GO:0035097). Bivalent genes enrichment was done by comparing our list to "3,868 bona-fide bivalent genes" in supplementary table No. 1 of (Mas et al., 2018). Since there's no formal list of bivalent genes for any species, and there's published diversity even within the same species, we chose to use Mas et al list of mouse bona fide bivalent since majority of them are also MLL2 targets. Enrichment calculation is explained in the statistical analysis section.

Functional enrichment analysis for comparison between different HS groups

Comparison between different HS groups was done on 11,679 genes after removal of "culturing" genes as explained in previous section. Upregulated and downregulated genes with padj < 0.05 between each HS treatment and the relevant control, were intersected using Venn diagram to check for unique and common genes between the treatments (Figures 5A-B). List of genes with no culturing effect was prepared for each treatment (Supplementary Table S7), and enrichment analysis for specific pathways was done using The Graeber Lab online calculator for

941 hypergeometric p value. Pathways analyzed: N00455: CDC25-Cell cycle G2/M (KEGG pathway), R-
942 BTA-69002 – DNA Replication Pre-Initiation (Reactome), GO:0007049: Cell cycle (MGI database),
943 GO:0060070: Canonical WNT signaling, GO 0048863: Stem cell differentiation, GO:0048468: Cell
944 development, GO:0009888: Tissue development, GO:0007492: Endoderm development,
945 GO:0007498: Mesoderm development, GO:0048762: Mesenchymal cell differentiation,
946 GO:0002526: Acute Inflammatory response, GO:1905517: Macrophage migration, GO:0032635.
947 Cytokine pathway list was taken from PathCards v5.7.551.0. This analysis was used in Figure 5.
948 Enrichment calculation is explained in the statistical analysis section.

949 **Additional analysis**

950 In order to mark the DEGs influenced by different heat shock treatments, KEGG pathway maps
951 were downloaded from KEGG pathway database and marked with colors for down (blue) and up
952 (red) regulated genes on each pathway (cell cycle - bta041100, adhesion molecules - bta04514,
953 axon guidance - bta04360, DNA replication - bta03030, Oxidative phosphorylation - bta00190,
954 Glycolysis - bta00010, Wnt signaling - bta04310). String datasets was used for functional protein
955 association networks. SVG formats were further processed in Inkscape graphic software 1.1.2.

956

957 **Statistical Analysis**

958 GraphPad Prism (La Jolla, CA, United States) was used for statistical analysis and visualization of
959 RT-PCR. $P < 0.05$ was considered statistically significant. For Enrichment analysis hypergeometric
960 p value was calculated using The Graeber Lab online calculator 2009 ©
961 (https://systems.crump.ucla.edu/hypergeometric/). Parameters used for hypergeometric test: N
962 (population size) = 27607; M (number of successes in population) = number of genes in the tested
963 pathway, (e.g., in MLL1-2 list contains total of 32 genes); s (sample size) = number of genes in
964 specific treatment or cluster; k (number of successes) = number of genes present from pathway
965 list in specific treatment or cluster.

966

967 **Tools and Database URLs:**

968 - IGV **(**https://software.broadinstitute.org/software/igv/**)**
969 - QualiMap **(**http://qualimap.conesalab.org/**)**
970 - RStudio Team (2020). RStudio: Integrated Development for R. RStudio, PBC, Boston,
971 (https://www.rstudio.com/)

- Ensembl BioMart (https://www.ensembl.org/info/data/biomart/)
- bioDBnet (https://biodbnet-abcc.ncifcrf.gov/)
- GSEA (http://software.broadinstitute.org/gsea/)
- g:Profiler (https://biit.cs.ut.ee/gprofiler/)
- Cytoscape (http://www.cytoscape.org/) - ClueGO application
- EpiFactors Database (https://epifactors.autosome.org/)
- MGI database (http://www.informatics.jax.org/vocab/gene_ontology/)
- The Graeber Lab online calculator (https://systems.crump.ucla.edu/hypergeometric/)
- BioVenn (https://www.biovenn.nl/index.php)
- Inkscape (https://inkscape.org/)
- String database (https://string-db.org/)

985 **RNA-seq analysis workflow**

- Cutadapt - Trimming adaptors and poly A in the reads
- FastQC - Quality Control of the reads
- STAR - Mapping reads to Bos_taurus.ARS-UCD1.2 genome
- HTSeq - Counting reads to features
- IVG - Visual exploration of aligned data
- QualiMap – Alignment evaluation

- **DESeq – Normalization of the counts and differential expression analysis (Attached supplementary File No.5):**
  - 27607 – Total number of genes
  - 16595 – Genes who have 5 counts at least in total
  - 3667 – Differentially expressed genes (DEGs) with padj<0.05 & log2(Fold Change)>1

GSEA Analysis

14205 human orthologs

Hallmarks

&

GO, KEGG

DEG analysis using g:Profiler and CluGo

3667 genes

padj < 0.05 &

log2(FC) > 1

GO, KEGG &

Reactome

Long term effects and comparison between HS groups

11679 genes with no culturing effect

Padj < 0.05 between HS and control, Venn diagram to see which genes are specific for which group and prepared gene lists per treatment

GO, KEGG and

Reactome

&

Specific pathways enrichment

986 **Supplementary Table 1:**

987 List of all bovine primers used in this study for gene expression analysis by RT-qPCR

Name	Target Gene	Sequence	Forward/Reverse
PSMB2	Proteasome subunit beta 2	GATGCGAAATGGTTATGAACTG	Forward
PSMB2	Proteasome subunit beta 2	AGGTTTCGGCGAGTGAAAT	Reverse
RPS9	Ribosomal protein S9	GAAGCTGATCGGCGAGTATG	Forward
RPS9	Ribosomal protein S9	GATCTTGGCCAGGGTGAAT	Reverse
CD29	Integrin beta 1	GCCAAGCAGATGAAAACAGA	Forward
CD29	Integrin beta 1	AATGTTGAATTTGTGCACCATC	Reverse
CD44	CD44	GTCCTATGCGGAAACCTCAA	Forward
CD44	CD44	GCCCACACCTTCTCCTACTG	Reverse
CD90	Thy-1	CGCCCTCCTGCTAACAGTC	Forward
CD90	Thy-1	GGCGTGGTGGTGGTATTCT	Reverse
CD105	Endoglin	TGGTCAGTAACGAGGTGGTCA	Forward
CD105	Endoglin	AGTGTGGGCTGAGGTAGAGG	Reverse
VIM	Vimentin	GATGGACAGGTTATCAACGAAACT	Forward
VIM	Vimentin	TCCTTCTTGCTGGTAGTATTTTGC	Reverse
KRT19	Keratin	CTTCCGCACCAAGTTTGAGAC	Forward
KRT19	Keratin	CTGCATCTCCAGGTCAGTCC	Reverse
Nanog	Nanog	CTCAGCTACAAGCAGGTGAAGA	Forward
Nanog	Nanog	TATTCCTCGGCCAGTTGTTT	Reverse
CD146	Melanoma cell adhesion molecule (MCAM)	TGGTCAGTAACGAGGTGGTCA	Forword
CD146	Melanoma cell adhesion molecule (MCAM)	AGTGTGGGCTGAGGTAGAGG	Reverse
HGF	Hepatocyte growth factore	CGAGGCCATGGTGCTATACT	Forword
HGF	Hepatocyte growth factore	TTCATAGTACTGTGGGCGCA	Reverse
POLH	DNA Polymerase Eta	TGTGGGCAGATGATGCTAAG	Forward
POLH	DNA Polymerase Eta	CCCGGTACTTGGTGAGGTTAG	Reverse
HSP27	Heat shock protein 27	CCCTGGACGTCAACCACTT	Forward
HSP27	Heat shock protein 27	CTCGTGCTTGCCAGTGATCT	Reverse
HSP90	Heat shock protein 90	GAGCAGTATGCCTGGGAGTC	Forward
HSP90	Heat shock protein 90	CCATTGGTTCTCCTGTGTCA	Reverse
MDM2	Murine Double Minute 2	GAACAAGAGACCCTGGTTAGA	Forward
MDM2	Murine Double Minute 2	CCTTCTGTGCACCAACAGACT	Reverse
CDK2	Cyclin Dependent Kinase 2	AGTACTGCCATACGAGAGATCT	Forward
CDK2	Cyclin Dependent Kinase 2	ACATCCAGCAGCTTGACAATAT	Reverse
CCNA	Cyclin A	CAGGACCAAGAAAGCCACTG	Forward
CCNA	Cyclin A	GTGGAGACTCAAAACTACCATCC	Reverse
PCNA	Proliferating cell nuclear antigen	TGTCTCCTTGGTGCAGCTAA	Forward
PCNA	Proliferating cell nuclear antigen	TTGGACATGCTGGTGAGGTT	Reverse

988

989 **Supplementary Table 2:** Samples used for RNA-seq

Sample Name	Total reads	Uniquely mapped reads (STAR)
ShortNT-1	54,230,074	89.51%
ShortNT-2	39,577,082	90.10%
ShortNT-3	28,420,067	90.32%
LongNT-1	38,872,317	90.03%
LongNT-2	25,950,940	90.11%
ShortHS-1	48,638,628	89.98%
ShortHS-2	26,125,462	89.93%
ShortHS-3	28,842,747	89.88%
ShortHS_Recovery-1	45,307,646	90.08%
ShortHS_Recovery-2	20,743,593	89.81%
LongHS-1	39,755,614	90.03%
LongHS-2	30,679,249	89.87%
LongHS-3	26,106,742	90.52%

990

991 **Supplementary Table 3:** Culturing conditions of the samples used in heat shock experiments

Treatment name	Temperature (^{o}C)	Time	Cell No. - Start	Cell No. - End
ShortNT	37°C	6h	250,000	329,212
ShortHS	40.5^{O}C	6h	250,000	320,365
ShortHS_Recovary	40.5^{O}C	6h	72,000	345,600
	37°C	66h		
LongNT	37°C	72h	42,000	344,400
LongHS	40.5^{O}C	72h	72,000	104,982

992

993

994

995

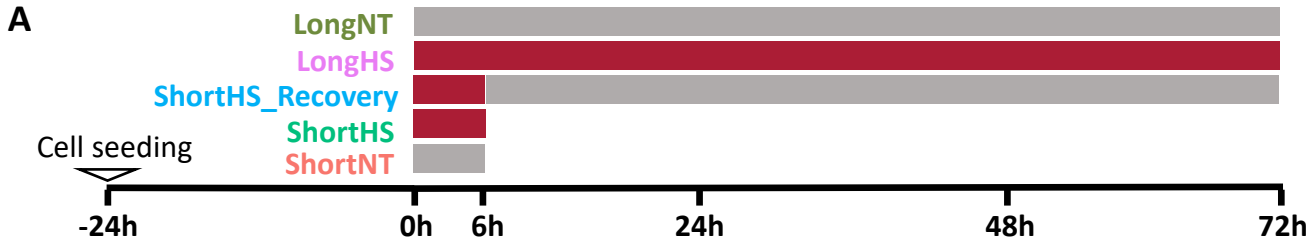
A
LongNT
LongHS
ShortHS_Recovery
ShortHS
ShortNT
Cell seeding
-24h
0h
6h
24h
48h
72h

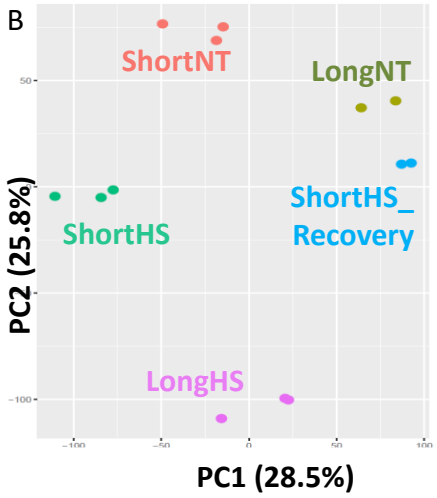
B
ShortNT
LongNT
ShortHS
ShortHS_
Recovery
LongHS
PC2 (25.8%)
PC1 (28.5%)

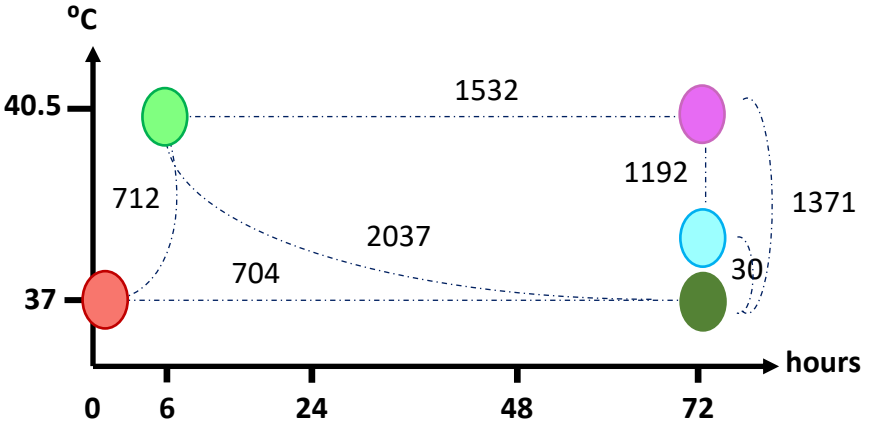
°C
40.5
37
1532
712
1192
1371
2037
704
30
hours
0
6
24
48
72

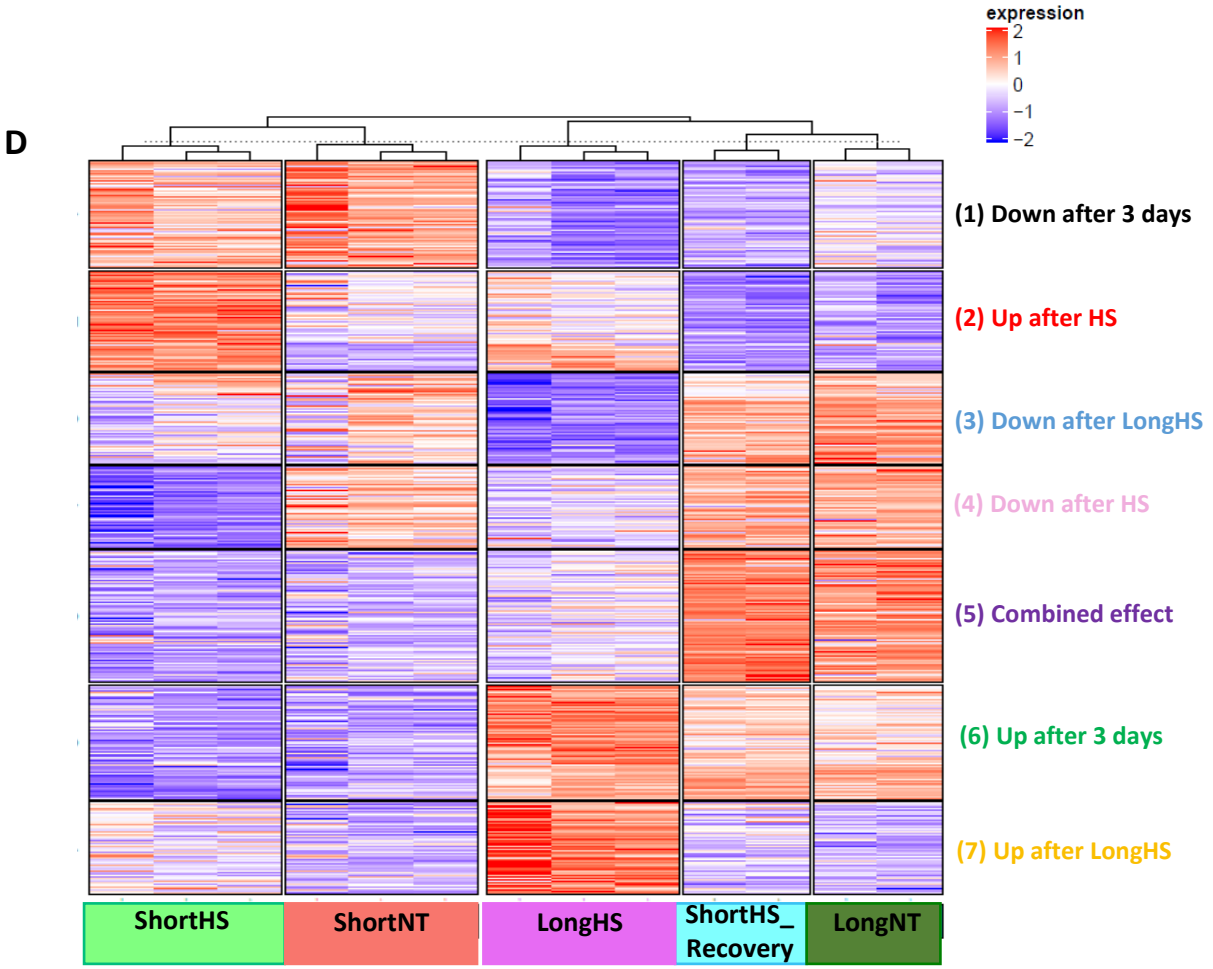
D
expression
2
1
0
−1
−2
(1) Down after 3 days
(2) Up after HS
(3) Down after LongHS
(4) Down after HS
(5) Combined effect
(6) Up after 3 days
(7) Up after LongHS
ShortHS
ShortNT
LongHS
ShortHS_
Recovery
LongNT

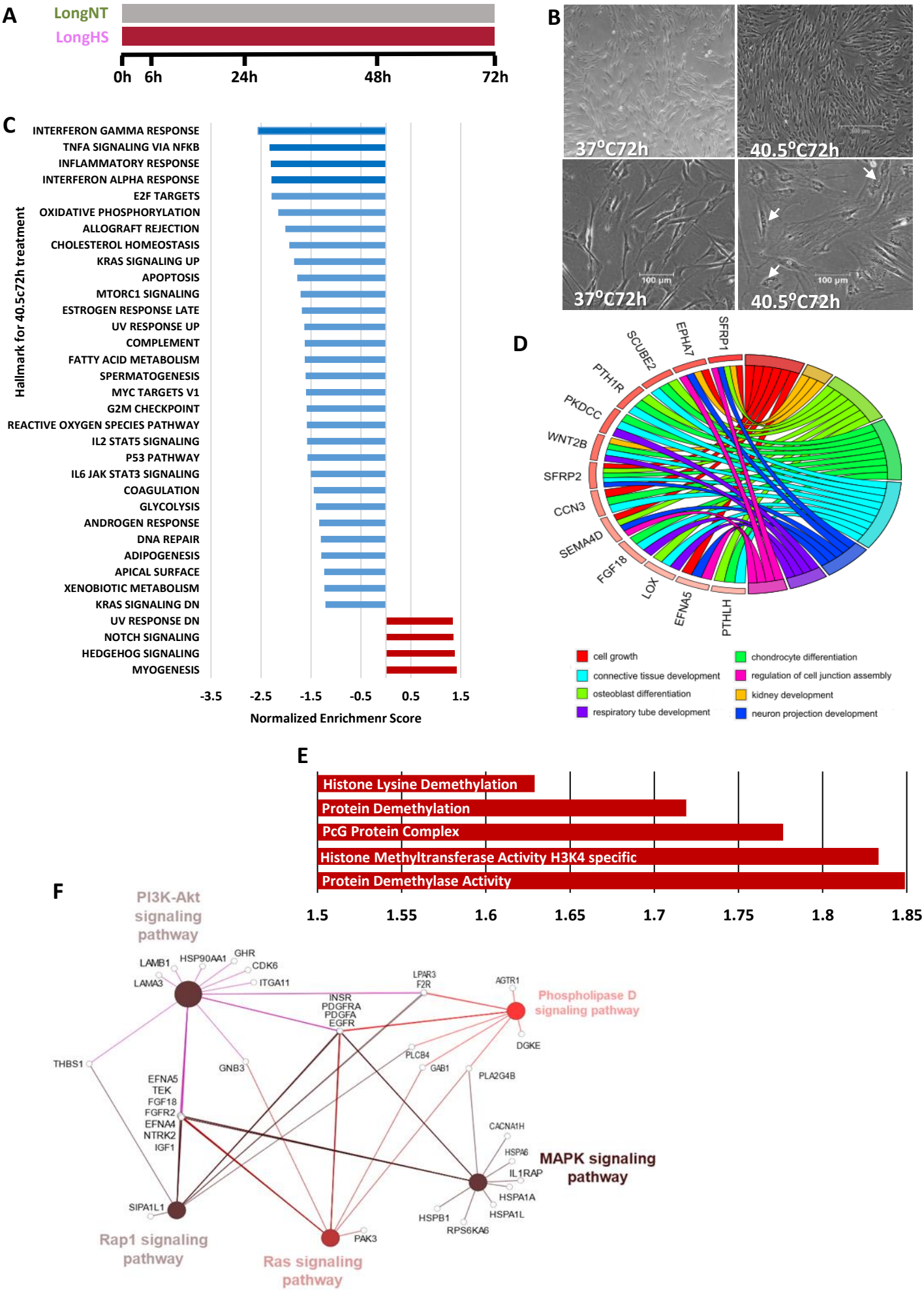
A
LongNT
LongHS
0h
6h
24h
48h
72h
B
37°C72h
40.5°C72h
37°C72h
40.5°C72h
100 µm
100 µm
C
Hallmark for 40.5c72h treatment
INTERFERON GAMMA RESPONSE
TNFA SIGNALING VIA NFKB
INFLAMMATORY RESPONSE
INTERFERON ALPHA RESPONSE
E2F TARGETS
OXIDATIVE PHOSPHORYLATION
ALLOGRAFT REJECTION
CHOLESTEROL HOMEOSTASIS
KRAS SIGNALING UP
APOPTOSIS
MTORC1 SIGNALING
ESTROGEN RESPONSE LATE
UV RESPONSE UP
COMPLEMENT
FATTY ACID METABOLISM
SPERMATOGENESIS
MYC TARGETS V1
G2M CHECKPOINT
REACTIVE OXYGEN SPECIES PATHWAY
IL2 STAT5 SIGNALING
P53 PATHWAY
IL6 JAK STAT3 SIGNALING
COAGULATION
GLYCOLYSIS
ANDROGEN RESPONSE
DNA REPAIR
ADIPOGENESIS
APICAL SURFACE
XENOBIOTIC METABOLISM
KRAS SIGNALING DN
UV RESPONSE DN
NOTCH SIGNALING
HEDGEHOG SIGNALING
MYOGENESIS
-3.5
-2.5
-1.5
-0.5
0.5
1.5
Normalized Enrichmenr Score
D
SFRP1
EPHA7
SCUBE2
PTH1R
PKDCC
WNT2B
SFRP2
CCN3
SEMA4D
FGF18
LOX
EFNA5
PTHLH
cell growth
connective tissue development
osteoblast differentiation
respiratory tube development
chondrocyte differentiation
regulation of cell junction assembly
kidney development
neuron projection development
E
Histone Lysine Demethylation
Protein Demethylation
PcG Protein Complex
Histone Methyltransferase Activity H3K4 specific
Protein Demethylase Activity
1.5
1.55
1.6
1.65
1.7
1.75
1.8
1.85
F
PI3K-Akt signaling pathway
LAMB1
HSP90AA1
GHR
CDK6
LAMA3
ITGA11
LPAR3
F2R
AGTR1
Phospholipase D signaling pathway
INSR
PDGFRA
PDGFA
EGFR
DGKE
THBS1
GNB3
PLCB4
GAB1
PLA2G4B
EFNA5
TEK
FGF18
FGFR2
EFNA4
NTRK2
IGF1
CACNA1H
HSPA6
IL1RAP
MAPK signaling pathway
HSPA1A
HSPA1L
HSPB1
RPS6KA6
SIPA1L1
PAK3
Rap1 signaling pathway
Ras signaling pathway

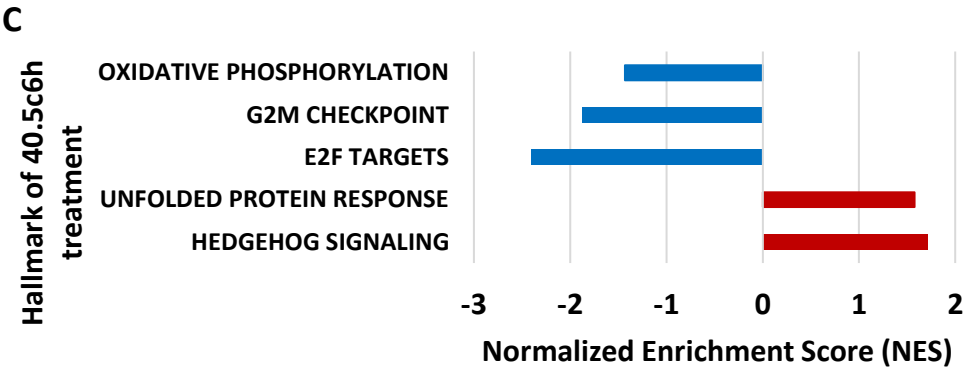

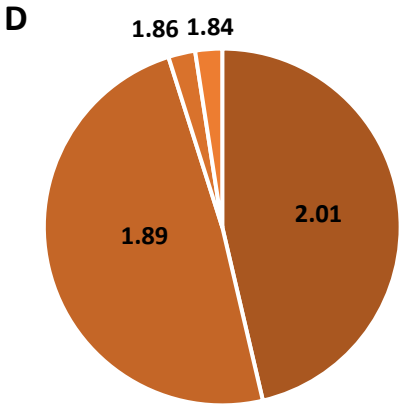

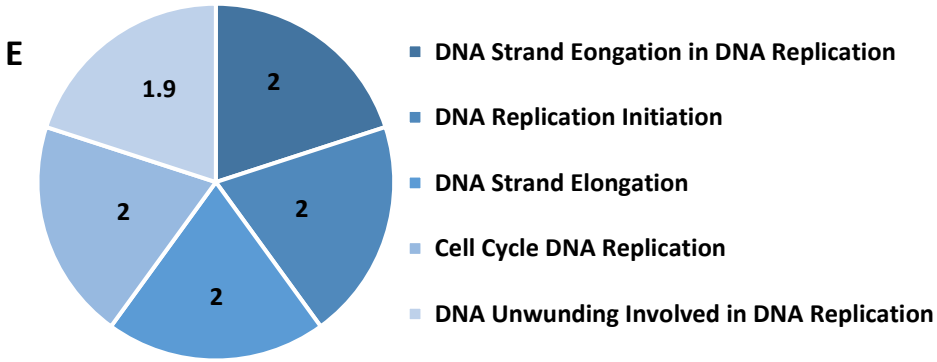

F

Term name	Term ID	P_{adj}
Protein processing in endoplasmic reticulum	KEGG:04141	1.720×10^{-9}
DNA-binding transcription activator activity	GO:0001216	1.222×10^{-2}
HSP90 chaperone cycle for steroid hormone receptors (SHR)	REAC:R-BTA-337...	2.349×10^{-4}
Regulation of HSF1-mediated heat shock response	REAC:R-BTA-337...	3.540×10^{-4}
Cellular response to heat stress	REAC:R-BTA-337...	3.540×10^{-4}
DNA replication initiation	GO:0006270	2.933×10^{-5}
organic acid catabolic process	GO:0016054	3.993×10^{-3}
carboxylic acid catabolic process	GO:0046395	1.330×10^{-2}
DNA-dependent DNA replication	GO:0006261	1.708×10^{-2}
small molecule catabolic process	GO:0044282	2.304×10^{-2}
DNA replication	KEGG:03030	1.031×10^{-3}
Cell cycle	KEGG:04110	1.126×10^{-3}
Tyrosine metabolism	KEGG:00350	2.121×10^{-2}
Glycine, serine and threonine metabolism	KEGG:00260	4.270×10^{-2}
DNA Replication Pre-Initiation	REAC:R-BTA-690...	2.363×10^{-3}
Metabolism of amino acids and derivatives	REAC:R-BTA-712...	3.758×10^{-3}
DNA Replication	REAC:R-BTA-693...	1.445×10^{-2}
Phenylalanine and tyrosine metabolism	REAC:R-BTA-896...	2.615×10^{-2}
Assembly of the pre-replicative complex	REAC:R-BTA-688...	2.615×10^{-2}

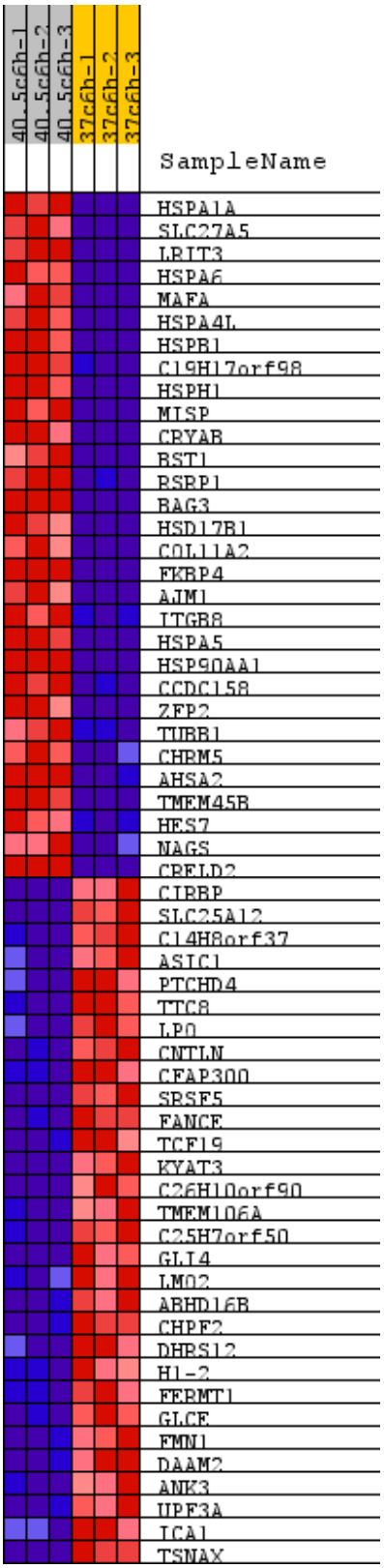

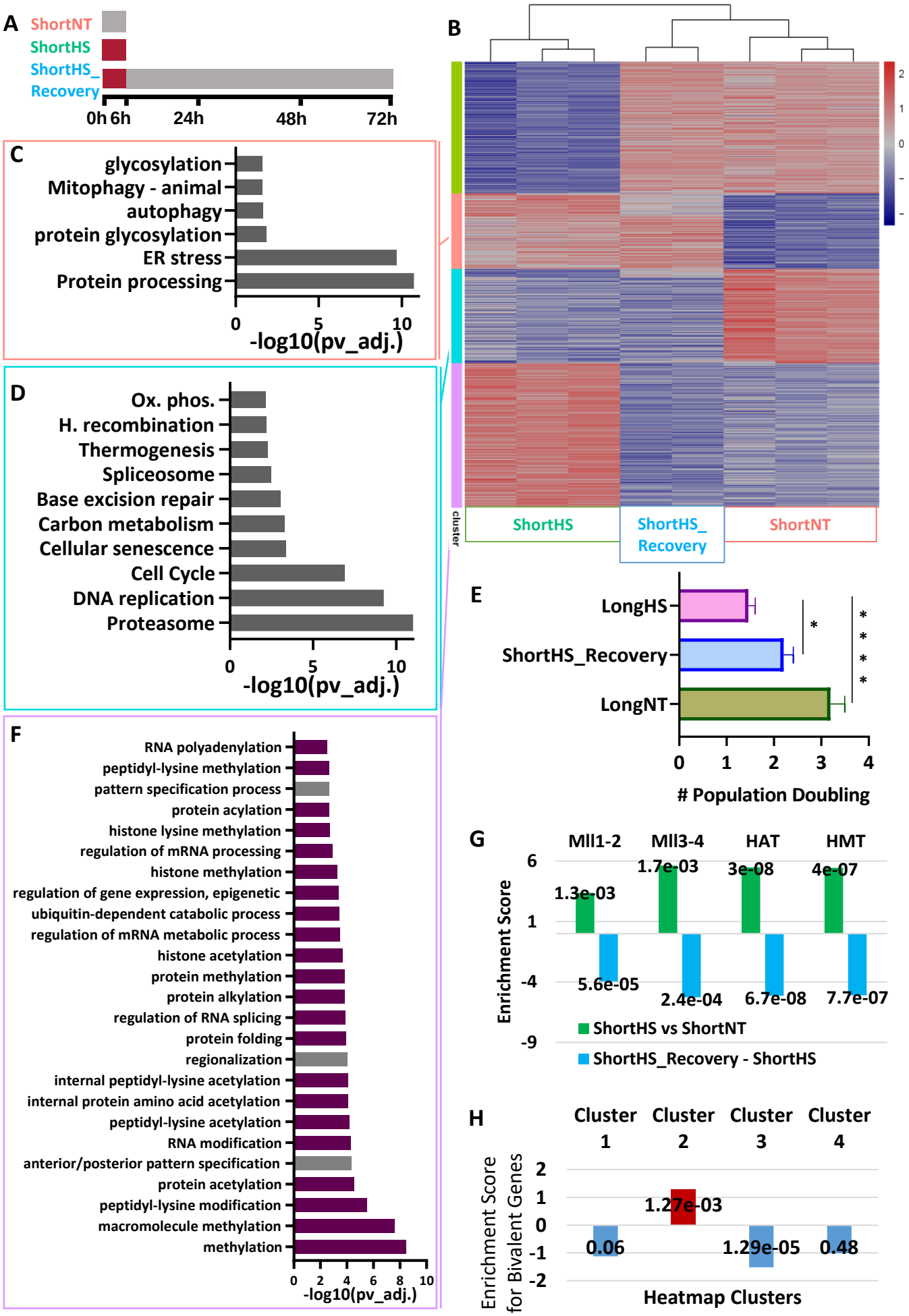
A
ShortNT
ShortHS
ShortHS_
Recovery
0h 6h
24h
48h
72h
B
cluster
ShortHS
ShortHS_
Recovery
ShortNT
C
glycosylation
Mitophagy - animal
autophagy
protein glycosylation
ER stress
Protein processing
0
5
10
-log10(pv_adj.)
D
Ox. phos.
H. recombination
Thermogenesis
Spliceosome
Base excision repair
Carbon metabolism
Cellular senescence
Cell Cycle
DNA replication
Proteasome
0
5
10
-log10(pv_adj.)
E
LongHS
ShortHS_Recovery
LongNT
*
*
*
*
0
1
2
3
4
Population Doubling
F
RNA polyadenylation
peptidyl-lysine methylation
pattern specification process
protein acylation
histone lysine methylation
regulation of mRNA processing
histone methylation
regulation of gene expression, epigenetic
ubiquitin-dependent catabolic process
regulation of mRNA metabolic process
histone acetylation
protein methylation
protein alkylation
regulation of RNA splicing
protein folding
regionalization
internal peptidyl-lysine acetylation
internal protein amino acid acetylation
peptidyl-lysine acetylation
RNA modification
anterior/posterior pattern specification
protein acetylation
peptidyl-lysine modification
macromolecule methylation
methylation
0
2
4
6
8
10
-log10(pv_adj.)
G
Mll1-2
Mll3-4
HAT
HMT
Enrichment Score
6
1
-4
-9
1.3e-03
1.7e-03
3e-08
4e-07
5.6e-05
2.4e-04
6.7e-08
7.7e-07
ShortHS vs ShortNT
ShortHS_Recovery - ShortHS
H
Cluster 1
Cluster 2
Cluster 3
Cluster 4
Enrichment Score for Bivalent Genes
2
1
0
-1
-2
1.27e-03
0.06
1.29e-05
0.48
Heatmap Clusters

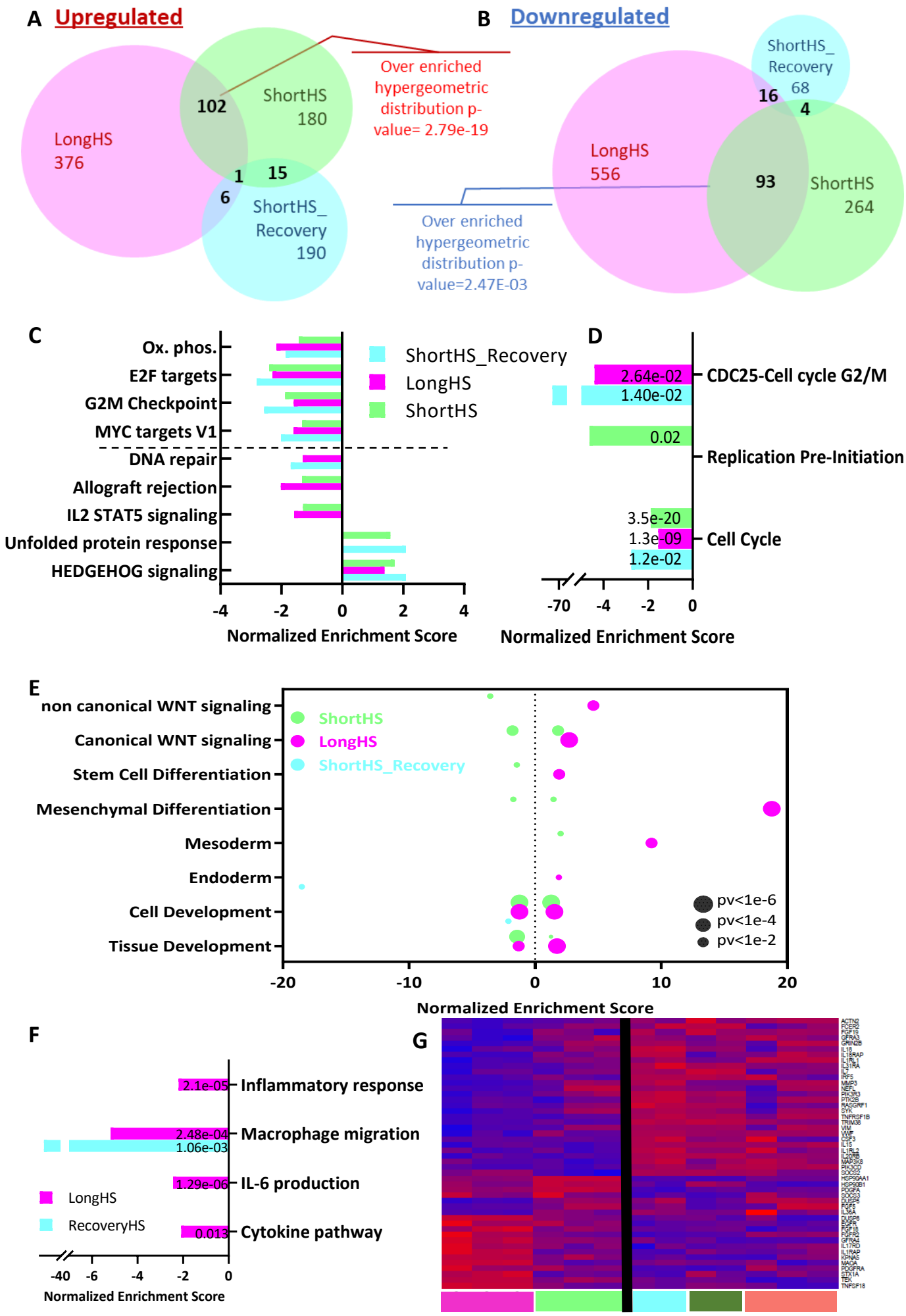
A Upregulated
LongHS
376
ShortHS
180
ShortHS_
Recovery
190
102
1
15
6
Over enriched hypergeometric distribution p-value= 2.79e-19
B Downregulated
LongHS
556
ShortHS_
Recovery
68
ShortHS
264
16
4
93
Over enriched hypergeometric distribution p-value=2.47E-03
C
Ox. phos.
E2F targets
G2M Checkpoint
MYC targets V1
DNA repair
Allograft rejection
IL2 STAT5 signaling
Unfolded protein response
HEDGEHOG signaling
ShortHS_Recovery
LongHS
ShortHS
-4
-2
0
2
4
Normalized Enrichment Score
D
2.64e-02
1.40e-02
CDC25-Cell cycle G2/M
0.02
Replication Pre-Initiation
3.5e-20
1.3e-09
1.2e-02
Cell Cycle
-70
-4
-2
0
Normalized Enrichment Score
E
non canonical WNT signaling
Canonical WNT signaling
Stem Cell Differentiation
Mesenchymal Differentiation
Mesoderm
Endoderm
Cell Development
Tissue Development
ShortHS
LongHS
ShortHS_Recovery
pv<1e-6
pv<1e-4
pv<1e-2
-20
-10
0
10
20
Normalized Enrichment Score
F
2.1e-05
Inflammatory response
2.48e-04
1.06e-03
Macrophage migration
1.29e-06
IL-6 production
0.013
Cytokine pathway
LongHS
RecoveryHS
-40
-6
-4
-2
0
Normalized Enrichment Score
G